Hydrogen-bonding in polymer blends

Shiao-Wei Kuo

Abstract Hydrogen bonding in polymer blends is a topic of great interest to polymer scientists because such systems have many potential applications. Introducing functional groups to one component to make it capable of forming hydrogen bonds to another, thereby enhancing the miscibility of otherwise immiscible blends, is one of the major achievements during the past 20 years of polymer science. The Painter–Coleman association model generally describes these interactions accurately. This Review discusses in detail the effects of hydrogen bonding on the miscibility and thermal properties of polymer blend systems.

Keywords Hydrogen bonds · Polymer blends · Miscibility · Glass transition temperature · Melting temperature · Crystallization

Nomenclature

AFM	Atomic force microscopy
PHB	Poly(3-hydroxybutyrate)
ACA	Vinyl alcohol-co-vinyl acetate
PHEMA	Poly(hydroxylethyl methacraylte)
BPA	Bisphenol A
PHPMA	Poly(hydroxylpropyl methacrylate)
CHEX	Cyclohexane
PHS	Poly(hydroxystryene)
DMA	Dynamic mechanic analysis
PLLA	Poly(l-lactide)
DMF	Dimethylformamide
PMA	Poly(methyl acrylate)
DSC	Differential scanning calorimetry
PMAAM	Poly(methyl methacrylamide)
EMAA	Ethylene-co-methacrylic acid
PMMA	Poly(methyl methacrylate)
IPP	Isopropyl phenol
PPzMA	Poly(phenyl methacrylate)
LiClO4	Lithium perchlorate
PPO	Poly(dimethyl phenylene oxide)
NMR	Nuclear magnetic resonance
PS	Poly(styrene)
PAA	Poly(acrylic acid)
PSOH	Poly(styrene-co-vinyl phenol)
PAS	Poly(acetoxystyrene)
PVA	Poly(vinyl alcohol)
PBMA	Poly(butyl methacrylate)
PVAc	Poly(vinyl acetate)
PBT	Poly(butylene terephathlate)
PVC	Poly(vinyl chloride)
PBzMA	Poly(benzyl methacrylate)
PVDF	Poly(vinylidene floride)
PCHMA	Poly(cyclohexyl methacrylate)
PVP	Poly(vinyl pyrrolidone)
PCL	Poly(ε-caprolactone)
P2VP	Poly(2-vinyl pyridine)
PDA	Poly(adipic ester)
P4VP	Poly(4-vinyl pyridine)
PDMS	Poly(dimethylsiloxane)
PVPh	Poly(vinyl phenol)
PECH	Poly(epichlorohydrin)
SAA	Styrene-co-acrylic acid
PEDEK	Poly(ether diphnyl ether ketone)
TEM	Transmission electron microscopy
PEEK	Poly(ether ether ketone)
THF	Tetrahydrofuran

S.-W. Kuo (✉)
Department of Materials Science and Optoelectronic Engineering,
Center for Nanoscience and Nanotechnology,
National Sun Yat-Sen University,
Kaohsiung 804, Taiwan
e-mail: kuosw@faculty.nsysu.edu.tw

PEMA   Poly(ethyl methacrylate)
XPS   X-ray photoelectron spectroscopy
PEO   Poly(ethylene oxide)
PEOx   Poly(2-ethyl-2-oxazoline)

Introduction

In recent years, much attention has been paid to the nature of hydrogen bonds and their effects on the microstructures and physical properties of various materials [1–6]. The classical example is water. It is now general recognized that the tetrahedral water cluster consists of 14 water molecules, the central 10 of which form a strong cluster and the remaining four form pentagons in the completed icosahedral cluster. The unusual properties of water arise from the ability of water molecules to form hydrogen bonds with various molecules and ions—and doing so in a tetrahedral geometry [7]. Other examples of hydrogen bonding systems in molecular biology are the hybridization of DNA duplexes [8] and the α-helix and β-sheet secondary structures of polypeptides, which are stabilized through intramolecular and intermolecular hydrogen bonds, respectively [9, 10]. In general, hydrogen bonding has a profound effect on the physical properties of polymer materials, including their melting temperature, glass transition temperature, dielectric constant, surface properties, and crystal structure, as well as the central concern of this review: the solubility and miscibility of polymer blends.

Polymer blending is a powerful route toward materials exhibiting property and cost performances superior to those of their individual components. In essence, three types of blends can be distinguished: completely miscible, partially miscible, and immiscible [11, 12]. In most cases, polymer blends are immiscible because of the high degrees of polymerization of their components; thus, the entropy term becomes vanishingly small and the miscibility becomes increasingly dependent on the nature of contribution of the enthalpic term. To enhance the formation of single-phase, miscible polymer blends, it is necessary to ensure that favorable specific intermolecular interactions exist between the two base components of the blend. Ideally, one polymer will possess donor sites on its chain; the other, acceptor sites. The most commonly observed interactions are generally acid/base types, namely hydrogen bonding, ion-dipole, π–π, or charge transfer interactions [13–19].

Much of our research in recent years has involved studies of intermolecular hydrogen bonding. Although, several excellent reviews exist on hydrogen-bonded polymer blends [20–26], this review mainly discusses our recent research efforts in this field.

Characterization of hydrogen bond

Hydrogen bond

The concept of the hydrogen bond being a directed, attractive interaction between an electron-deficient hydrogen atom and a region of high electron density has been reviewed thoroughly in several books [27] and reviews [28]. In general, a hydrogen bond is defined as a system in which a hydrogen atom lies between two atoms A and B—ideally in the linear form A–H⋯B—with the distance between the nuclei of A and B being considerably shorter than the sum of the van der Waals radii of A and B and the diameter of the proton (i.e., the formation of a hydrogen bond leads to contraction of the A–H⋯B system). The atoms A and B are usually highly electronegative, such as F, O, and N atoms. Hydrogen bonds are also defined by their effects on the properties of a material or its molecular characteristics. Covalent bonds have strengths of the order of 50 kcal/mol; among noncovalent bonds, van der Waals attraction is on the order of 0.2 kcal/mol, whereas hydrogen bonding is somewhat stronger, lying in the range 1–10 kcal/mol in various solvents at room temperature. Note that the strength of a particular hydrogen bond is highly dependent on the nature of the solvent employed. Polar solvents significantly decrease a hydrogen bond's strength because they also participate in hydrogen bonding interactions with the hydrogen bond donor and acceptor units. Therefore, the supramolecular chemistry of hydrogen-bonded polymers is mostly investigated in nonpolar solvents, such as linear and cyclic alkanes, toluene, dichloromethane, and chloroform.

Characterization of hydrogen bonds

The most widely used experimental methods for characterizing hydrogen bonds are: (1) infrared (IR) and Raman spectroscopy, which can provide information about the stretching and deformation vibrations of the A–H bonds and acceptor groups; (2) electronic absorption and fluorescence spectroscopy in the ultraviolet (UV) and visible regions, which reveal the effect of hydrogen bond formation on the electronic levels of the participating molecules; (3) solid or liquid state nuclear magnetic resonance (NMR) spectroscopy, which can reveal the effect of hydrogen bond formation on the chemical shift of the signal of the A–H unit [29]; and (4) X-ray photoelectron spectroscopy (XPS), which can reveal specific hydrogen bonding interactions in polymer blends. The development of a new peak or shoulder is often observed in XPS spectra when the chemical environment of an atom in a polymer blend is perturbed as a result of a specific interaction [30–38].

Among these methods, the most sensitive and inexpensive by far is IR spectroscopy, although solid state NMR

spectroscopy has recently been used to clarify the phase behavior and morphology of polymer blends featuring hydrogen bonds. The ^{13}C NMR chemical shift and line shape in cross-polarization and magic angle spinning (CP/MAS) spectra can be used to identify the chemical environments of the carbon atoms in the blend, because the chemical shift and line shape are highly sensitive to the local electron density. Thus, if a specific interaction affects the local electron density, a change in chemical shift can usually be observed [39–42]. Figure 1 presents an example of this chemical shift behavior for the C=O and OH groups in the ^{13}C NMR spectrum of a PVPh/PVP blend [43]. The variation in the observed chemical shift (≒ 1.2 ppm) of the C=O carbon atom reveals the existence of a specific interaction between the PVPh and PVP segments. Hydrogen bonding in polymer blends can affect the chemical environment of neighboring molecules, causing a downfield chemical shift. For example, the OH-substituted carbon atom (C-6) in the phenolic unit of pure PVPh resonates at 153.2 ppm; a downfield shift of 2.8 ppm is observed in the PVPh/PVP=20/80 blend, implying the presence of a strong intermolecular interactions between the OH groups of PVPh and the C=O groups of PVP. Such behavior is widely interpreted as evidence for interactions occurring between blend components.

In addition to the changes in the chemical shifts and line shapes in solid state NMR spectra, the scale of the miscibility of a polymer blend can be estimated from the proton spin-lattice relaxation times in the rotating frame $(T_{1\rho}^{H})$ measured in the solid state [44–50]. For example, we used the spin lattice relaxation time in the rotating frame determined through solid state NMR spectroscopy to explore the homogeneity and phase behavior of polymer blends and diblock copolymers of PVPh/P4VP. Table 1 lists the values of $T_{1\rho}(H)$ for diblock copolymers, blends, and blend complexes of PVPh/P4VP [51]. A single composition-dependent value of $T_{1\rho}(H)$ was obtained for each of these systems, suggesting that they are homogeneous on the scale where spin-diffusion occurs within the time $T_{1\rho}(H)$.

In addition, the $T_{1\rho}(H)$ values for the blends were higher than those for the two individual pure polymers, but those of the diblock copolymers and blend complexes were lower. These results imply that diblock copolymers have relatively smaller domain sizes than do their corresponding blends, indicating that the degrees of homogeneity of diblock copolymers are relatively higher than those of their blends. As a result, the shorter $T_{1\rho}(H)$ relaxation times of block copolymers reflect the greater rigidity of their polymer chains and their enhanced glass transition temperature (T_g). By comparing polymer blends of PAA/PVP with the complex of PAA/PVP, the resultant $T_{1\rho}(H)$ values reveal the same trend; i.e., the value of $T_{1\rho}(H)$ of the complex of PAA/PVP is shorter than that of the corresponding blend
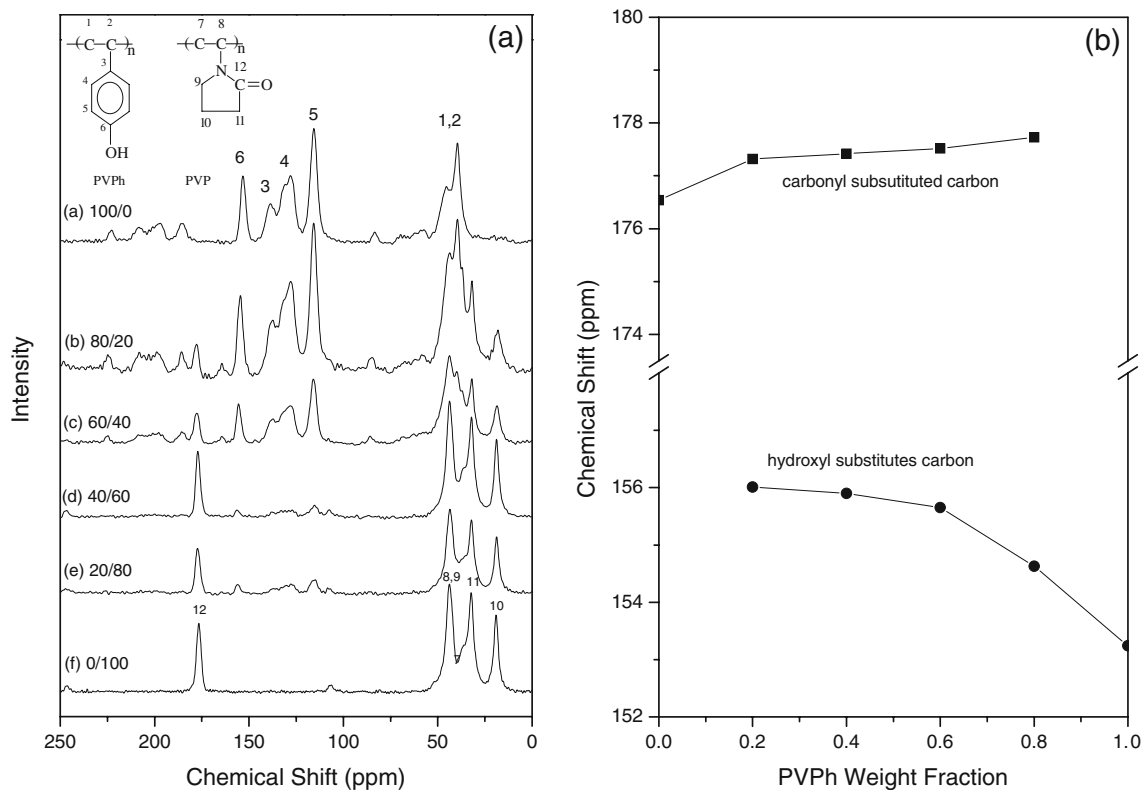
Fig. 1 **a** [13]C CPMAS spectra, **b** chemical shift of carbonyl group (*filled square*), the hydroxyl substituted carbon (*filled circle*) in the PVPh/PVP blends

Table 1 Relaxation times, $T_{1\rho}^{H}$, for blends, blend complex, and diblock copolymers at the magnetization intensities of 40 and 115 ppm

PVPh /P4VP 40 ppm	$T_{1\rho}^{H}$ (ms)	PVPh-b-P4VP	$T_{1\rho}^{H}$ (ms)	PVPh/P4VP[a] 115 ppm	$T_{1\rho}^{H}$ (ms)	PVPh-b-P4VP	$T_{1\rho}^{H}$ (ms)
–	–	–	–	100/0	8.79		8.79
30/70	7.80	28-b-72	6.55	30/70	10.70	28-b-72	7.07
50/50	8.40	50-b-50	6.92	50/50	9.40	50-b-50	7.09
70/30	8.69	90-b-10	5.60	70/30	9.10	90-b-10	5.53
Complex	7.26	–	–	Complex	7.11	–	–
0/100	7.56	0/100	7.56	–	–	–	–

[46]. Unlike NMR spectroscopy-based analyses, further on in this review we will discuss how IR vibrational spectroscopy allows us not only to measure of the strength of the hydrogen bond interactions but also—more crucially—to determine the number of free and hydrogen-bonded groups.

Association model approach

Although association models have been used for many years to describe, for example, the mixing of alcohols with simple hydrocarbons, the miscibility behavior of polymer blends has only recently attracted significant attention in polymer science. For nonpolar polymer blends, the miscibility behavior can be roughly estimated using the Flory–Huggins [52] polymer solution theory:

$$\frac{\Delta G_N}{RT} = \frac{\Phi_1}{N_1} \ln \Phi_1 + \frac{\Phi_2}{N_2} \ln \Phi_2 + \Phi_1 \Phi_2 \chi_{12} \qquad (1)$$

where Φ and N denote the volume fraction and the number of segments; χ_{12} represents the so-called Flory–Huggins interaction parameter, calculated using Hilderbrand's solubility parameter, written in terms of $\chi_{12} = (\delta_1 - \delta_2)^2 / RT$; and the subscripts 1 and 2 refer to the blend compounds. In the case of high-molecular-weight polymers, the values of N_1 and N_2 are very much greater than 1 and, consequently, the first two entropy terms become vanishingly small and the miscibility becomes increasingly dependent on the nature of the contribution of the enthalpic term. It is well known, however, that Eq. 1 it is incapable of predicting either the lower critical solution temperature (LCST) or the polymer–polymer miscibility. During the past 20 years, many modifications of the classical Flory–Huggins theory have been proposed; including Sanchez's statistical thermodynamics polymer blend model [53], Paul's binary interaction model [54], and Painter and Coleman's association model [55]. In general, the behavior of most hydrogen bonded polymer blends is predicted well by the Painter–Coleman association model.

Painter and Coleman suggested adding an additional term to the simple Flory–Huggins expression to account for the free energy of hydrogen bond formation upon mixing two polymers:

$$\frac{\Delta G_N}{RT} = \frac{\Phi_1}{N_1} \ln \Phi_1 + \frac{\Phi_2}{N_2} \ln \Phi_2 + \Phi_1 \Phi_2 \chi_{12} + \frac{\Delta G_H}{RT} \qquad (2)$$

where ΔG_H denotes the free energy change contributed by hydrogen bonding between the two components, which can be estimated using Fourier transform infrared (FTIR) spectroscopy. This equation neglects the change in free volume and other complications. Here we provide a simple example to illustrate the character of this approach and to facilitate a direct comparison with other methods of treatment. Consider the situation where one of the components of the mixture consists of molecules such as phenol (i.e., low-molecular-weight, non-polymeric species) that contain only one functional group capable of hydrogen bonding. The equilibrium equation for self-association can be described as follows:

$$B_1 + B_1 \xleftrightarrow{K_2} B_2 \qquad (3)$$

$$B_h + B_1 \xleftrightarrow{K_B} B_{h+1} (h > 2) \qquad (4)$$

where K_2 and K_B are defined as

$$K_2 = \frac{\Phi_{B_2}}{2\Phi_{B_1}^2} \qquad (5)$$

$$K_B = \frac{\Phi_{B_{h+1}}}{\Phi_{B_h} \Phi_{B_1}} \frac{h}{h+1} \qquad (6)$$

For the competing equilibrium

$$B_h + A_1 \xleftrightarrow{K_A} B_h A \qquad (7)$$

where unit A makes no distinction between forming a hydrogen bond to a dimer or to an h-mer, we obtain

$$K_A = \frac{\Phi_{B_h A}}{\Phi_{B_h} \Phi_{A_1}} \frac{hr}{h+r} \qquad (8)$$

where K_2 and K_B are the self-association constants for "dimer" and "multimer" formation, respectively, of B; K_A is the inter-association constant for the interaction between A

and B_h; r is equal to V_A/V_B, i.e., the ratio of the segmental molar volume; Φ_{Bh} is the volume fraction of the chains of length h; and Φ_{Ai} is the volume fraction of the chains of length i at any instant in time. The stoichiometric relationships are simply obtained from material balance considerations. The total volume fraction of all the A and B units present in the mixture is given by

$$\Phi_B = \Phi_{B_1} + \sum_{h=2}^{\infty} \Phi_{B_h} + \sum_{h=1}^{\infty} \Phi_{B_hA}\left(\frac{h}{h+r}\right) \tag{9}$$

$$\Phi_A = \Phi_{A_1} + \sum_{h=1}^{\infty} \Phi_{B_hA}\left(\frac{r}{h+r}\right) \tag{10}$$

Therefore, the total volume fraction of a self-associating polymer B and an inter-associating polymer A can be extended as follows:

$$\Phi_B = \Phi_{B_1}\left[\left(1 - \frac{K_2}{K_B}\right) + \frac{K_2}{K_B}\left(\frac{1}{(1-K_B\Phi_{B_1})^2}\right)\right]$$
$$\times \left[1 + \frac{K_A\Phi_{A_1}}{r}\right] \tag{11}$$

$$\Phi_A = \Phi_{0A}$$
$$+ K_A\Phi_{0A}\Phi_{B_1}\left[\left(1 - \frac{K_2}{K_B}\right) + \frac{K_2}{K_B}\left(\frac{1}{(1-K_B\Phi_{B_1})}\right)\right] \tag{12}$$

Figure 2 highlights the free energy of the mixing equation, which can be considered as consisting of three major contributions [20]. The combinatorial entropy—a very small, but nonetheless favorable, contribution to the

free energy of mixing—is contained in the first two logarithmic terms; Φ_A and Φ_B are the volume fractions of polymers A and B, respectively, in the blend and M_A and M_B are the corresponding degrees of polymerization. Thus, the free energy of mixing is dominated by the balance of the last two terms, $\chi\Phi_A\Phi_B$, which is an unfavorable contribution derived from physical forces, and $\Delta G_H/RT$, a favorable contribution derived from hydrogen bonding or so-called "chemical" forces. The positive contribution from the physical forces is determined using a Flory-type χ parameter that is, in turn, estimated from solubility parameters calculated from the molar attraction and molar volume constants of non-hydrogen-bonded groups.

The negative contribution from chemical forces is determined from equilibrium constants and enthalpies of hydrogen bond formation, which are derived from IR spectroscopic data to describe the self- and inter-associations and the distribution of hydrogen-bonded species in the polymer blend.
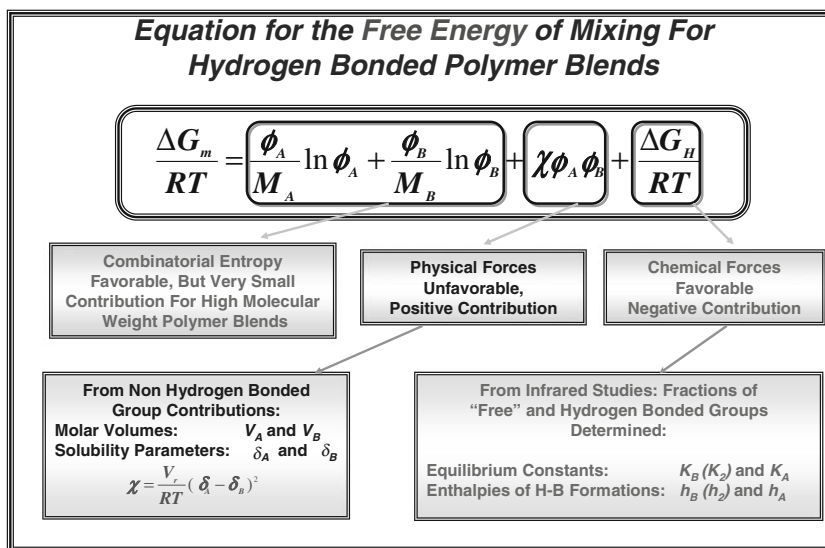
Measurement of hydrogen bonds using IR spectroscopy

In this section, we discuss how IR spectroscopy can be used to determine the number or fraction of functional groups that are either hydrogen bonded or free, and how this information can, in turn, be used to determine self- and inter-association equilibrium constants.

Self-association equilibrium constant

For a variety of reasons, the most important of which will be discussed later, the equilibrium constants that describe the self-association of polymers containing OH groups have been estimated from analogues of low molar mass. Molecules containing OH groups, such as phenol, isopropyl

Fig. 2 A summary of the various contributions to the free energy of mixing equation

Equation for the Free Energy of Mixing For Hydrogen Bonded Polymer Blends

$$\frac{\Delta G_m}{RT} = \frac{\phi_A}{M_A}\ln\phi_A + \frac{\phi_B}{M_B}\ln\phi_B + \chi\phi_A\phi_B + \frac{\Delta G_H}{RT}$$

Combinatorial Entropy Favorable, But Very Small Contribution For High Molecular Weight Polymer Blends

Physical Forces Unfavorable, Positive Contribution

Chemical Forces Favorable Negative Contribution

From Non Hydrogen Bonded Group Contributions:
Molar Volumes: V_A and V_B
Solubility Parameters: δ_A and δ_B
$$\chi = \frac{V_r}{RT}(\delta_A - \delta_B)^2$$

From Infrared Studies: Fractions of "Free" and Hydrogen Bonded Groups Determined:
Equilibrium Constants: $K_B(K_2)$ and K_A
Enthalpies of H-B Formations: $h_B(h_2)$ and h_A

phenol, and ethyl phenol, self-associate in the condensed state through the formation of hydrogen-bonded hydroxyl–hydroxyl dimers and higher multimers, as illustrated in Fig. 3 [20].

Here, we choose 4-isopropylphenol (IPP) in cyclohexane (CHEX) as an example to calculate the self-association equilibrium constant. CHEX was selected as the solvent because it does not possess any fundamental vibration frequencies in the OH stretching region of the IR spectrum. Nevertheless, solutions containing large quantities of CHEX inevitably reveal overtone and combination bands that interfere with the analytical range of interest. To eliminate these signals' contributions from the spectra of IPP/CHEX mixtures, the spectrum of the pure CHEX was digitally subtracted, as indicated in Fig. 4 [56], to reveal a relatively sharp signal for free OH stretching.

Figure 5 displays IR spectra of various IPP/CHEX mixtures [56]. Upon increasing the concentration of IPP beyond 0.01 M, the effect of self-interaction of dimers and, especially, multimers becomes increasingly noticeable. To calculate the self-association equilibrium constant [57], we measured the fraction of the free monomers at each concentration of IPP.

The intensity (absorbance) of the isolated OH band at 3,620 cm^{-1}, I, is related to the absorptivity coefficient (ε), concentration (c), and path length (l) in terms of the Beer–Lambert law ($I=\varepsilon \times l \times c$). The value of the absorptivity coefficient ε is determined by plotting I/cl versus c; a value of 31.1 was obtained using the equation $\lim_{c \to 0} \left| \frac{I}{cl} \right| = \varepsilon$, as indicated in Fig. 6 [56].

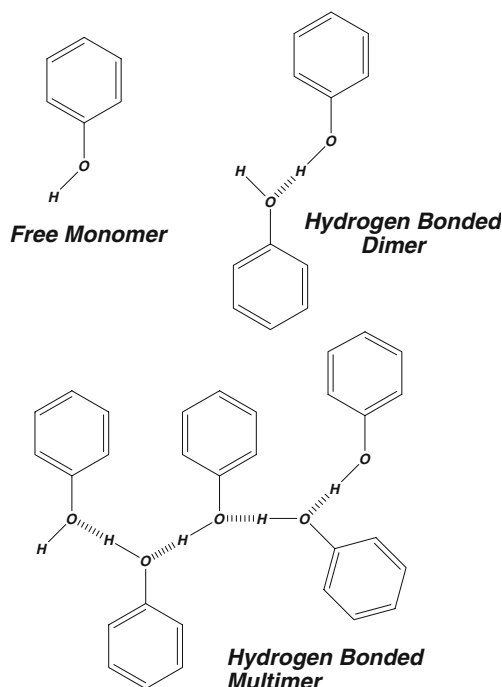**Fig. 3** Self-association hydrogen bonding of phenol

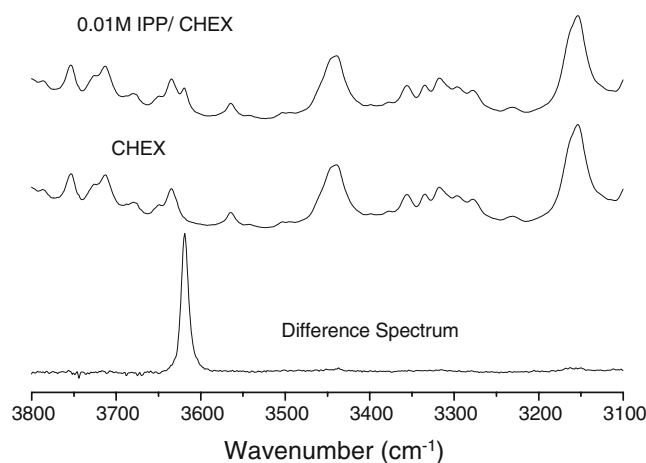**Fig. 4** Infrared spectra of IPP/CHEX recorded in the region from 3,100–3,700 cm^{-1}

The experimental fraction of free monomers (f_m^{OH}) and the value of $\varepsilon = (I/cl)$ at each given concentration of IPP was calculated. When the concentration of IPP increased, the fraction of free OH groups decreased gradually. There are two equilibrium constants that describe the self-association of IPP OH groups: one for the formation of dimers (K_2) and one for multimeric complexes (K_B), as described by Eqs. 3–6.

We used Eq. 13 [20] to obtain the best fit of K_2 and K_B for IPP:

$$f_m^{OH} = \frac{\phi_{B_1}}{\phi_B} = \left[\left(1 - \frac{K_2}{K_B} \right) + \frac{K_2}{K_B} \left(\frac{1}{1 - (K_B \phi_{B_1})^2} \right) \right]^{-1}$$

(13)

where ϕ_B is the total volume fraction of B and α_{B_1} is the volume fraction of non-hydrogen-bonded species. Figure 7 displays the best fit for IPP ($K_2 = 28.3$ L mol^{-1}; $K_B = 72.6$ L mol^{-1}). We assume that the values of K_2 and K_B for OH-containing polymers are the same as those obtained for their model compounds (e.g., for phenolic resin, where we employ 2,4-dimethylphenol as a model).

As a result, the equilibrium constants are simply scaled to the molar value of the specific repeat unit of the polymers using the expression $K_i^{Polymer} = 100 K_i^* / V_{segment}$. Table 2 lists typical values for some OH-containing polymers [58–61].

Inter-association equilibrium constant

Inter-association refers to hydrogen-bonded association between systems featuring two different functional groups, e.g., a simple mixture of ethylphenol with *p*-tolyl acetate. At equilibrium, free and hydrogen bonded phenolic dimers and multimers still exist, as illustrated in Fig. 3, but additional species are now formed through the capping of
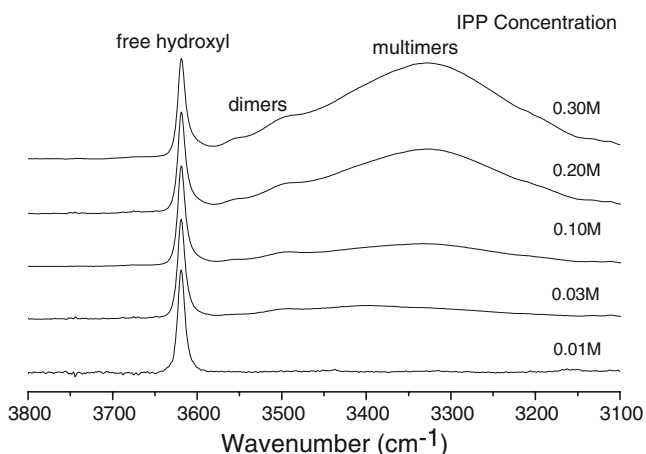
Fig. 5 Absorption bands for hydroxyl groups of IPP in CHEX at various concentrations
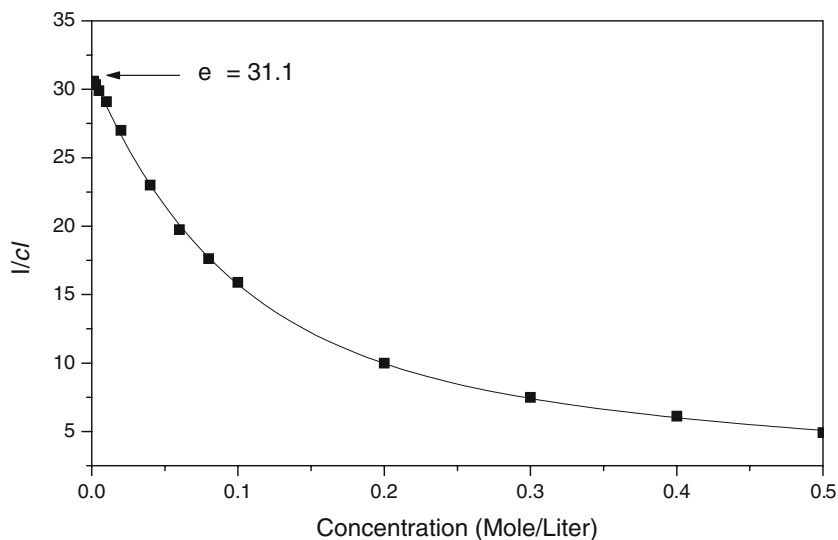
hydrogen-bonded phenolic chain-like structures via a hydrogen bond to the C=O groups of *p*-tolyl acetate molecules. The precise distribution of all of these species is now dependent upon the composition of the mixture, the temperature, and the equilibrium constants that describe both self- and inter-association.

Based on PCAM, the inter-association equilibrium constant K_A can be calculated using two methods. The first method, reported by Coggesthall and Saier (C&S) [62], involves calculation of the hydrogen bonding association constant, K_a (units: L mol^{-1}), which is expressed by the following equation (14):

$$K_a = \frac{1 - f_m^{OH}}{f_m^{OH}\left(C_A - \left(1 - f_m^{OH}\right)C_B\right)} \quad (14)$$

where C_A and C_B denote the concentrations (mol L^{-1}) of *p*-tolyl acetate and 2,6-dimethylphenol, respectively, and f_m^{OH} represents the fraction of free OH units of 2,6-dimethyl-

phenol, defined as $f_m^{OH} = I/I_0$, where $I_0 = a_F^{OH} \times b \times c$ and I is the intensity of the free hydroxyl band. The term a_F^{OH}, which is related to the absorptivity coefficient of 34.2 for phenol, was obtained previously by Hu et al. [57]; b is the path length (0.05 mm); c is the concentration.

Figure 8 presents the OH group absorptions of a 2,6-dimethylphenol solution in CHEX containing various concentrations of *p*-tolyl acetate [63].

The intensity of the free OH absorption at 3,620 cm^{-1} decreased upon increasing the concentration of *p*-tolyl acetate. The absolute intensity of this signal is considered to be a measurement of the number of free OH groups in the mixture, based on Eq. 14. Therefore, the value of f_m^{OH} for a solution of ethylphenol containing various concentrations of *p*-tolyl acetate can be calculated from the values of K_a. The intrinsic inter-association constant K_a (10.67 L mol^{-1}) is obtained by extrapolating the *p*-tolyl acetate concentration to zero. The value of K_a is transformed into K_A by dividing the molar volume of the phenolic repeat unit (0.083 L mol^{-1} at 25 °C) [58]. The value of inter-association equilibrium constant K_A yielded through this procedure was 128.6.

The second method for determining K_A is a numerical method according to the PCAM based on the fraction of hydrogen-bonded C=O groups. Figure 9 displays the C=O stretching region of the IR spectra of phenoic/PAS blends as a function of their composition [63].

The C=O stretching frequency is split into two bands at 1,760 and 1,730 cm^{-1}, which are assigned to free and hydrogen-bonded C=O groups, respectively. The fraction of hydrogen-bonded C=O groups can be calculated by using an appropriate absorptivity ratio ($a_R = a_{HB}/a_F = 1.5$), as has been discussed previously [29]. In that investigation, the authors attempted to use another approximate method proposed by Coleman et al. to obtain K_A, the equilibrium constant describing the association of A with B, expressed

Fig. 6 The determination the value of absorptivity coefficient

Fig. 7 The best fit for determining of the self-association equilibrium constants of IPP
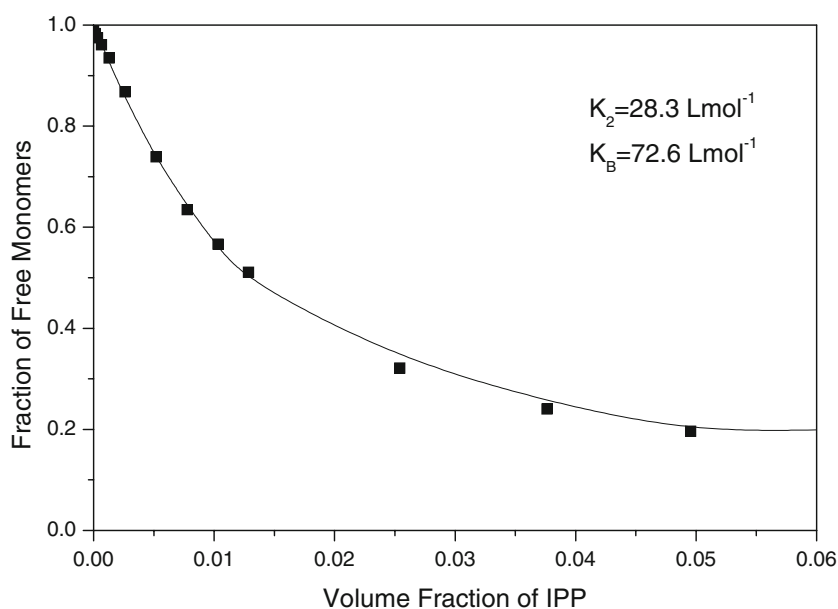
by Eqs. 11 and 12. In addition, the values of K_B and K_2 of the pure phenolic are 52.3 and 23.3, respectively, at 25 °C [58]. To calculate the inter-association constants (K_A), a methodology using a least-squares method has been employed widely [64]. Combining these previously determined values of K_B and K_2 with a given value for K_A and an appropriate value of r, we can calculate the root value of Φ_{B_1}. The fraction of hydrogen-bonded C=O groups as a function of the volume fraction of phenolic is then simply given by the expression $1 - [\Phi_{A_1}/\Phi_A]$. The value of K_A is employed to determine the best fit of the experimental data for polymer blends using a least-squares method. Figure 10 presents plots of the experimental data and theoretically predicted curves as a function of the composition; it

demonstrates the ability of PCAM to predict the degree of hydrogen bonding of the C=O group [53]. Clearly, the value of K_A (128.6) obtained from the model compound is greater than that for the polymer blend (64.6) because of several factors, such as the chain connectivity effect, intramolecular screening, and functional group accessibility [65–75].

The experimental values exhibit excellent agreement, however, with the values predicted for the polymer blend (K_A=64.6) for the hydrogen-bonded C=O groups. Thus, we consider the inter-association constant K_A of 64.4 for the phenolic/PAS blend to be a valid value. Therefore, the inter-association equilibrium constants determined for the polymer blend and the model compound differ on account of the

Table 2 Self-association equilibrium constants for some hydroxyl containing polymers

Material	Molecular structure	Self-association equilibrium constant	
		K_2	K_B
Phenolic resin		23.3	52.3
Phenoxy		14.4	25.6
Poly(vinylphenol)		21.0	66.8
Poly(vinyl alcohol)		26.7	44.1

Fig. 8 FTIR spectra of the hydroxyl stretching region of 0.02 M 2,4 dimethylphenol containing various *p*-tolyl acetate concentrations
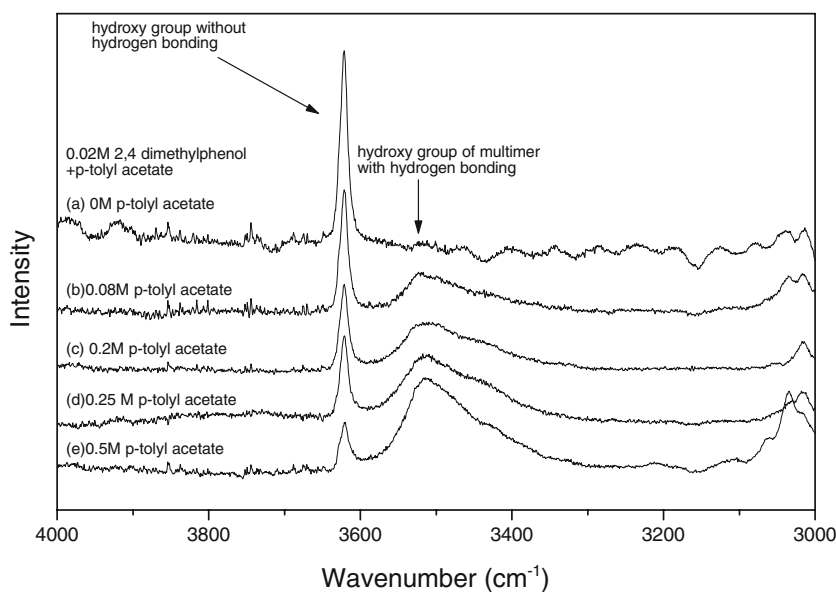
effects of intramolecular screening and functional group accessibility.

Factors influencing hydrogen bonding

Although these self and inter-association equilibrium constants cannot be obtained independently from their mixtures, the relative magnitudes of the inter and self-association equilibrium constants are, fortunately, more important when determining the dominant contributions to the free energy of mixing, rather than their individual absolute values [20]. If inter-association is strongly favored over self-association, the polymer blend is expected to be miscible; for example, the PVPh/PVP blend system, where K_A/K_B is equal to 100 [43]. Conversely, if self-association is stronger than inter-association, the blend tends to be immiscible or partially miscible; for example, the PVPh/PAS blend system [76]. The following subsections list the various factors that influence the hydrogen bonding strength.
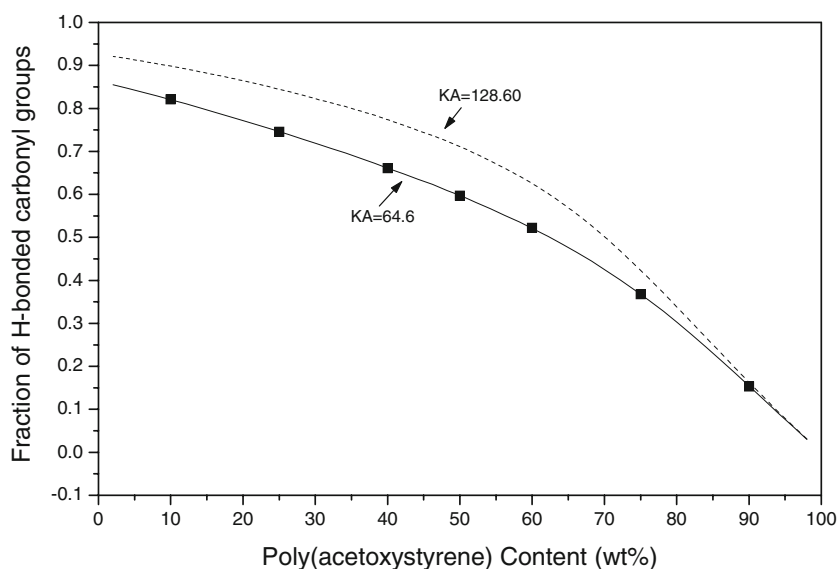
Intramolecular screening

The intramolecular screening effect is a consequence of chain connectivity. The covalent linkage between polymer segments causes an increase in the number of same-

Fig. 9 FTIR spectra at carbonyl region for phenolic/PAS blends
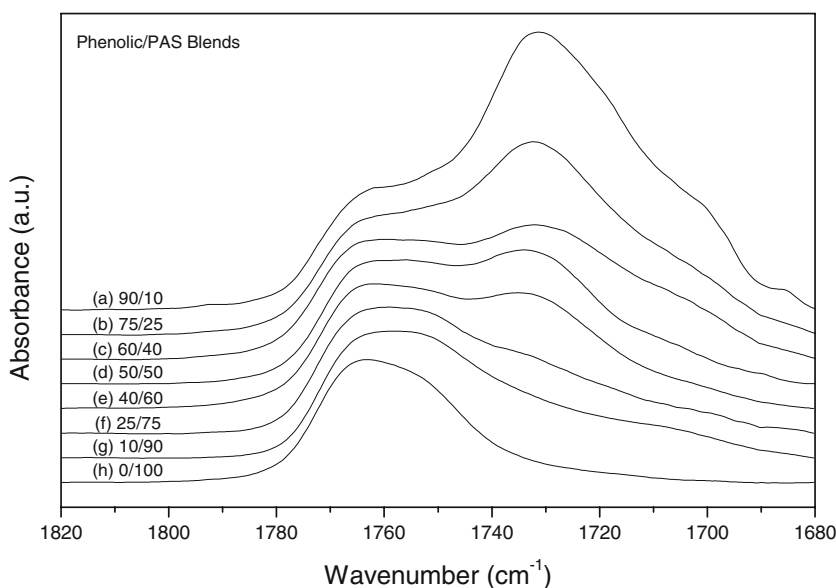
Fig. 10 FT-IR data (*filled square*), theoretical values from C&G method (*broken line*) and from PCAM (*solid line*)

polymer-chain contacts as a result of the polymer chains bending back on themselves; thus, the number of inter-association hydrogen bonds per unit volume in the polymer blend will be lower than that for the model compound. Figure 11 illustrates schematically the intramolecular screening effect of a polymer blend, with contributions from both short- and long-range screening effects [20, 75].

For an infinite chain, γ is surprisingly large, approaching 0.38 in the melt state; for real chains, however, the value is closer to 0.3 [65]. Moreover, the spacing between the functional groups along a polymer chain and the presence of bulky side groups can also significantly reduce the inter-association hydrogen bonding per unit volume, as a result of a so-called functional group accessibility effect [67].
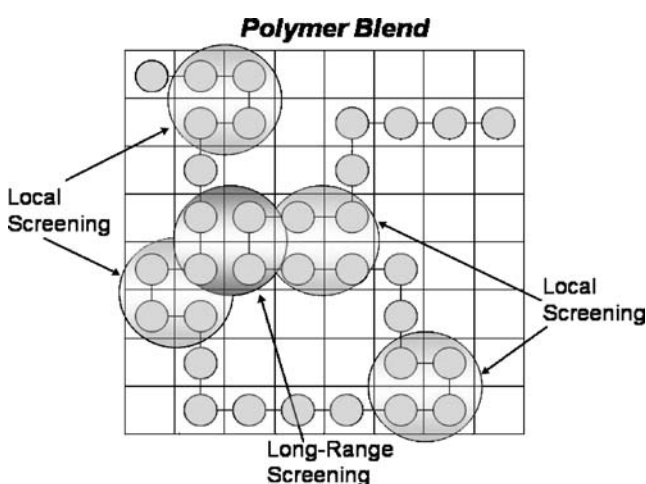
Fig. 11 Schematic illustration of local and long range contact in polymer that lead to screening effect

This effect is also considered to be the origin of steric crowding and shielding [68].

Functional group accessibility

Here we consider the measurement of the number of hydrogen bonds in random polymer blends in which the hydrogen bonding functional groups are separated along the chain by non-hydrogen bonding segments (inert diluent segments, such as polyethylene or polystyrene units). We use as an example the PSOH/PAS blend system [76]. The inter-association equilibrium constants K_A yielded using the C&S procedure (model compound) and the PCAM were 134.1 and 43.1, respectively, for this polymer blend system. In general, the inter-association constant of a polymer blend based on model compounds can be determined, as described by Coleman et al., as follows [67]:

$$K_A^{\mathrm{Std}} = K_A^{\infty} - \left(\frac{C_A}{R_A^0 + R_A} + \frac{C_B}{R_B^0 + R_B} \right) \qquad (15)$$

where R_A^0 and R_B^0 denote the molar volumes of the respective homopolymers; R_A and R_B represent the average molar volume between the A and B groups; C_A and C_B are fitting constants; and K_A^{∞} represents the intramolecular screening effect using an appropriate γ-value of 0.30 for a polymer blend [65]. Therefore, the inter-association constant is given by

$$K_A^{\infty} = K_A^{\mathrm{model}}(1 - \gamma) \qquad (16)$$

In this case, K_A^{∞} has a value of 93.87 (i.e., 134.1×0.7, dimensionless units). Using values of C_A and C_B of 1,630 and 4,100, respectively, as reported previously by Coleman et al. [67] for blends of PVPh and PVAc, because of their

similar structures to PAS and PVAc, Eq. 15 can be expressed as a function of R_A and R_B for the PSOH/PAS blend:

$$K_A^{std} = 93.87 - \left(\frac{1,630}{128.6 + R_A} + \frac{4,100}{100 + R_B} \right) \quad (17)$$

Using values of R_A and R_B of 0, we obtain a value of K_A for the PVPh/PAS blend system of 40.19. This value is very close to that obtained from the numerical method for the polymer blend, indicating that the thermodynamic properties in a polymer blend can be predicted from analogous model compounds after taking into account the effects of intramolecular screening and functional group accessibility.

Acidity of hydrogen bond donor

Recently, we investigated the effect of the chemical structure of the proton-donating polymer on the strength of the hydrogen bonds in binary blends with PCL [77]. We used DSC and FTIR spectroscopic analyses to investigate the hydrogen bonds formed between PCL and phenolic resin, PVPh, and phenoxy resin. In Fig. 12, it is clear that the degree of hydrogen bond formation with PCL follows the order phenolic/PCL > PVPh/PCL > phenoxy/PCL. Furthermore, the inter-association equilibrium constants and relative K_A/K_B ratios followed the same order as those calculated from PCAM [77].

Basicity of hydrogen bond donor

Kwei et al. investigated the intermolecular hydrogen bonding in poly(4-ethenyl phenolmethylsiloxane) (PEPS) blends with hydrogen bond acceptors (P4VP, PVP, PDMA, and SAN) of various strength [78]. The hydrogen bond strength followed the order P4VP > PVP > PDMA > SAN. Furthermore, they also compared the blending of PVPh with P4VP, PEO, and PBMA; the order of hydrogen bonding strength was P4VP > PEO > PBMA [79]. Based on our own findings, the inter-association equilibrium constants between PVPh and several hydrogen bonding acceptors have the following values: PVP=6,000; P4VP= 1,200; PEO=288; PCL=90; PHB=66; PVAc=58; PMMA= 37; PLLA=10 [20, 29, 77, 80–83]. Clearly, the chemical structure of the group accepting the hydrogen bond has great impact, as has been discussed in detail elsewhere [84].

Steric hinderance

Phenolic is completely miscible with P2VP and P4VP in the amorphous phase over the entire range of compositions because of strong hydrogen bonding between the OH groups of phenolic and the pyridyl rings of P2VP and P4VP [85]. The characteristic to be emphasized in these examples is the influence of the position of the nitrogen atom in the pyridyl ring. The IR spectral data indicate that P4VP has a greater ability to form hydrogen bonds with phenolic than does P2VP, presumably because steric hindrance of the nitrogen atoms in P2VP affects the formation of intermolecular hydrogen bonds. In addition, the inter-association equilibrium constant for the phenolic/ P4VP blend is greater than that of the phenolic/P2VP blend, confirming that P4VP has a greater ability to form hydrogen bonds than does P2VP. We also investigated how the position of the nitrogen atom of the pyridyl rings in these polymers is a characteristic that influences their coordination properties with $ZnClO_4$ [86]. The data obtained from FTIR, XPS, and solid state NMR spectroscopies indicated that P4VP is better than P2VP at

Fig. 12 The relationship between experimental data and theoretical prediction by PCAM of hydrogen bonded fraction of carbonyl group within various PCL blend systems: phenolic/ PCL (*filled square*), PVPh/PCL (*filled circle*), phenoxy/PCL (*filled triangle*)
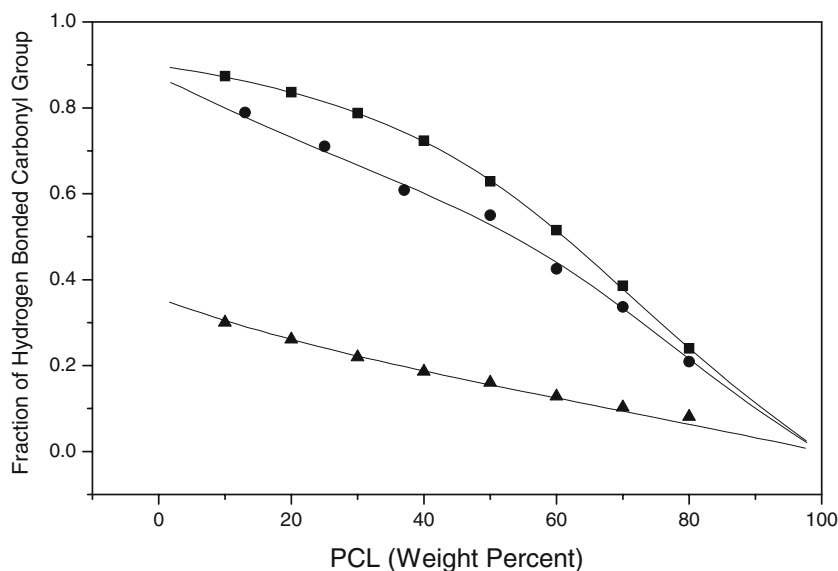
interacting with the zinc ions because of steric hindrance at the nitrogen atoms of P2VP.

Bulk of the side group

Painter et al. studied the hydrogen bonding in blends of PVPh copolymers with a series of poly(*n*-alkyl methacrylate)s (PAMAs) having various side chain lengths [66]. They found that the inter-association equilibrium constant was a suitable measure of the accessibility of the C=O groups, which decreased as the length of the side chain increased. They interpreted these results as providing evidence for the bulky side groups of the acrylates limiting the formation of hydrogen bonds in the blends. In addition, Coleman et al. also studied the effects of chain connectivity and steric crowding on the extent of hydrogen bonding in polymer solutions [67].

Temperature

In general, the enthalpy of hydrogen bond formation is negative; thus, the inter-association equilibrium constant and the number of the hydrogen bonds both decrease upon increasing the temperature. For example, Fig. 13 illustrates the FTIR spectra of the phenolic/PAS=50/50 blend measured at temperatures ranging from 25 to 180 °C [63].

The intensity of the signal for the hydrogen-bonded C=O groups decreased upon increasing the temperature, suggesting that intermolecular hydrogen bonding weakened and the number of hydrogen bonds decreased. As expected, the inter-association equilibrium constant in PVPh/PVAc blends [66] and the fraction of hydrogen-bonded pyridyl
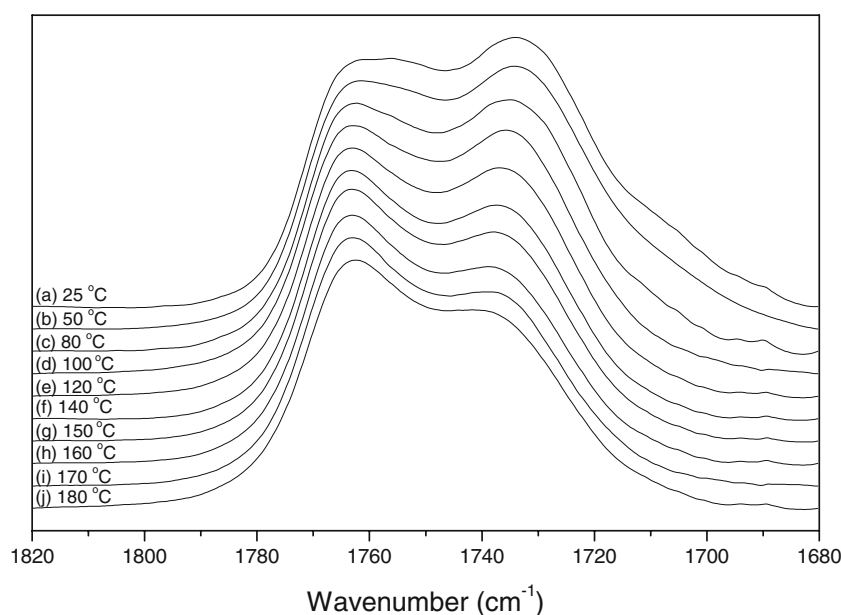
rings in phenolic/P4VP blends dropped upon increasing the temperature [85].

For multicomponent hydrogen bonding systems containing different competing acceptor groups, the different enthalpies of the various hydrogen bond formation processes can markedly affect the overall equilibrium constant. For example, quantitative analysis of the fraction of hydrogen-bonded C=O groups over the temperature range from 25 to 170 °C for the PVPh-*co*-PMMA/PEO=40/60 blend indicated a decreased from 25 to 50 °C and a subsequent increase upon further increasing the temperature [44]. The same phenomenon was observed by Coleman et al. in poly(vinylphenol-*co*-*n*-butyl methacrylate) and the styrene-*stat*-2-vinyl pyridine blend system [87]. Although this observation seems counterintuitive, the van't Hoff relationship ($K=-\Delta h/RT+C$) allows us to plot the values of the equilibrium constants as a function of the temperature from 25 to 200 °C, as shown in Fig. 14 [44].

The equilibrium constants K_A and K_C represent the competition between hydroxyl–ether inter-association and hydroxyl–carbonyl self-association, respectively; these values change with temperature at different rates. We observe that K_A equals K_C at ca. 70 °C, implying that an equivalent number of these interactions exists at this temperature. In contrast, K_C exceeds K_A at temperatures above 70 °C. Therefore, the observation that the fraction of hydrogen-bonded C=O groups increases with increasing temperature can be explained by the PCAM.

The fraction of hydrogen bonds formed with a semi-crystalline polymer should increase with an increase in temperature because the crystalline phase inhibits the formation of intermolecular hydrogen bonds. For example,

Fig. 13 FTIR spectra recorded at various temperatures for phenolic/PAS=50/50 blend

(a) 25 °C
(b) 50 °C
(c) 80 °C
(d) 100 °C
(e) 120 °C
(f) 140 °C
(g) 150 °C
(h) 160 °C
(i) 170 °C
(j) 180 °C

Wavenumber (cm⁻¹)

Fig. 14 Equilibrium constant values as a function of temperature from 25 to 200 °C
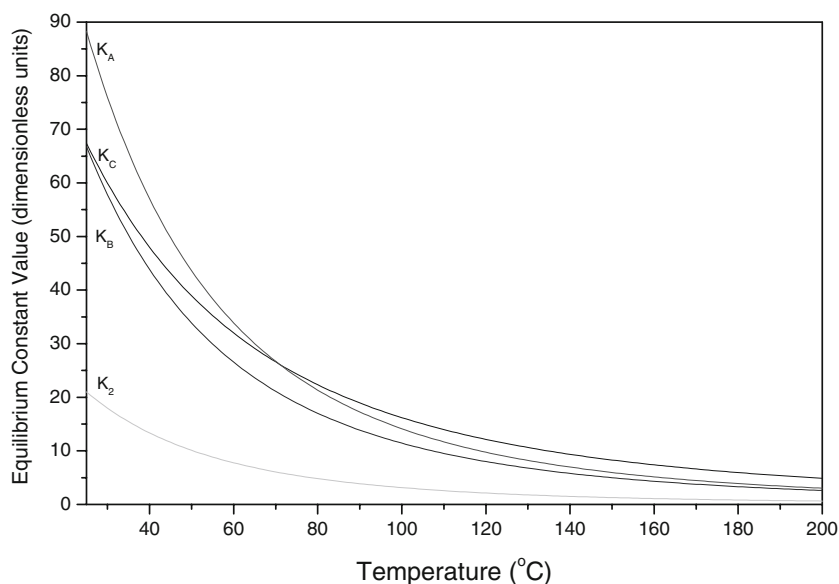
in the case of iPHB/catechin, the existence of strong hydrogen bonds was evident at 190 °C, i.e., above the melting temperature of iPHB, but they could not be detected at room temperature using FTIR spectroscopy [88]. Furthermore, in PVPh/PMMA blends, the fraction of hydrogen bonds was enhanced significantly upon increasing the temperature and annealing because temperatures above T_g increase the motion of the side chains and backbones and, thus, favor the formation of hydrogen bonds [89].

Miscibility enhancement through hydrogen bonding

To obtain a one-phase system using a polymer blend, it is usually necessary to ensure that favorable specific intermolecular interactions exist between the two or more base components of the blend. There is much interest in preparing miscible polymer blends in which one or both of the polymers are random copolymers [90–93]. Several copolymer/homopolymer and copolymer/copolymer blends are miscible over certain ranges of composition and temperature, even though their respective constituent homopolymers are pairwise immiscible, with no specific interactions existing in the blend systems because of the so-called "copolymer repulsion effect" [94, 95]. The overall interaction energy in these blend systems can be obtained using a binary interaction model based on the Flory–Huggins lattice theory, which can predict the effect of the copolymer composition on the miscibility of these blends [96]. The presence of hydrogen bonding usually enhances the miscibility of polymer blends because it generally provides a significant contribution to the free energy of mixing. For example, polystyrene (PS) is immiscible with

many other polymers because it lacks the functional groups necessary for strong noncovalent interactions. In generally, the miscibility of an immiscible blend can be enhanced by introducing to one of the polymers a functional group capable of forming intermolecular contacts with the other [97]. In general, there are three methods for enhancing the miscibility of an immiscible blend through hydrogen bonding: (1) incorporating a hydrogen bonding monomer on the main chain, (2) taking advantage of the inert diluent segment effect, and (3) forming a ternary polymer blend; we discuss each of these approaches in detail in the following subsections.

Incorporating a hydrogen bonding monomer on the main chain

PS is immiscible with phenolic resin; miscibility between phenolic resin and a styrene-rich copolymer can be achieved, however, after introducing acetoxystyrene units into the PS main chain (i.e., forming PS-*co*-PAS, the acetoxyphenyl units of which can form hydrogen bonds with the phenolic resin) [98]. We have used PCAM to predict whether a miscibility window exists for phenolic/PS-*co*-PAS blends. In Fig. 15, the weight fraction of phenolic resin in the blend is plotted against the mole percent of styrene in the PS-*co*-PAS copolymer. Phenolic resin was predicted to be completely miscible for phenolic/PS-*co*-PAS=50/50 blends in which the PAS content is greater than 40 mol%. Indeed, this model provided an accurate prediction of the miscibility window when compared with our experimental results based on DSC analyses.

In addition, we have also investigated blends of PCL and PSOH containing various vinylphenol contents; although
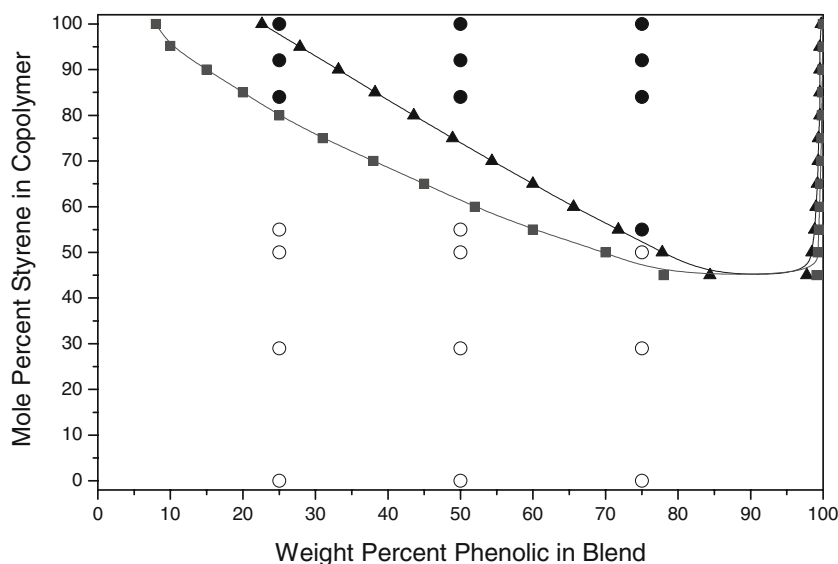
PS is immiscible with PCL, differential scanning calorimetry (DSC) analyses revealed that copolymers containing greater than 13 mol% vinylphenol were fully miscible with PCL [99]. In contrast, the Painter–Coleman association model and the binary interaction model predict that the critical vinylphenol content for the blend to be miscible is 0.1 mol% of the PSOH copolymer. The discrepancy between the experimental results and the theoretical predictions is probably caused by a significant free volume increase in this blend system, as analyzed using Kovacs' free volume theory [100].

Poly(4-vinylpyridine) (P4VP) is also immiscible with PS, but miscibility can be achieved for this system after introducing PVPh units into the PS main chain. When the PVPh content is more than 50 mol%, the copolymer is miscible with P4VP over the entire range of blend compositions; in contrast, if the styrene copolymer contains only 20–30 mol% of VPh units, miscibility is achieved only for blends that are rich in P4VP [101]. Similar to P4VP, poly(vinylpyrrolidone) (PVP) is also immiscible with PS; its blends become miscible when 11 mol% or more of PVPh is incorporated into the PS main chain, because hydrogen bonding interactions occur between the C=O groups of PVP and the OH groups of PVPh [102, 103]. A further example is that of PS and PEMA (or PMMA), where the incorporation of a certain amount of PVPh into the PS main chain enhances the miscibility of the blend [104].

Recently, a supramolecular polymer blend was prepared from a pair of immiscible polymers: poly(butyl methacrylate) (PBMA) and PS. A urea of guanosine (UG) and 2,7-diamido-1,8-naphthyridine (DAN), which form an exceptionally strong quadruply hydrogen-bonded complex [105], were presented at 1–10 mol% along the main backbones of PBMA and PS, respectively. Blends containing different weight ratios of the polymers and mole percentages of the recognition units were characterized using AFM and DSC experiments, which revealed no isolated domains and a single glass-transition temperature [106].

Inert diluent segment effect

As mentioned in "Factors influencing hydrogen bonding", hydrogen-bonded polymer blends are unlikely to be miscible if the self-association constant is stronger than the inter-association constant; in this case, the blend tends to be immiscible or partially miscible. For example, in the PVPh/PAS blend system, the incorporation of an inert diluent moiety (such as styrene) into the PVPh chain renders the modified polymer miscible with PAS; copolymers containing 16–51 mol% vinylphenol were fully miscible with PAS [76]. This behavior is caused by the incorporated styrene units within the PVPh chain reducing the strength of the self-association of PVPh and increasing the strength of the inter-association of the PVPh and PAS segments. Another example is that of PVPh/PCHMA blends, which exhibit two-phase behavior because of the PVPh component's strong self-associated hydrogen bonds. Miscibility has been observed for the blends, however, when a high content of styrene is copolymerized with PVPh [107]. Similar results have been observed for blends of bisphenol-A polycarbonate (BAPC) and tetramethyl bisphenol-A polycarbonate (TMPC) with PS-co-PVPh copolymers. BAPC is miscible with PS-co-PVPh over the range of ca. 45–75 mol% OH groups in the copolymer; TMPC has a somewhat wider miscibility window when blended with PS-co-PVPh [108]. The blend miscibility is probably driven by attractive intermolecular interactions between the OH groups of the PSOH. The large positive values of the segment interaction energy density parameters

($B_{\text{st-HS}}$), calculated from the group contribution approach, indicate that intramolecular repulsive interactions might also play a role in promoting the blend miscibility.

These examples all suggest that incorporating an inert diluent moiety (such as styrene) into PVPh results in a miscible blend system through a reduction of the degree of self-association (i.e., an increase in the ratio K_A/K_B) of the PVPh component in the blend. In fact, this phenomenon can also be explained by considering the copolymer repulsion effect [94, 95]. The enthalpy of mixing is usually responsible for miscibility because the contribution from the entropy change for a polymer blend is usually insignificant. For a binary mixture of a homopolymer A with a copolymer C_yD_{1-y}, the expression for the enthalpy of mixing is given by Eq. 18:

$$\frac{\Delta H_M}{V} = B\Phi_1\Phi_2 \tag{18}$$

where V is the total volume of the mixture, Φ_1 and Φ_2 are the respective volume fractions, and y is the molar fraction of component C in the copolymer. The value of B in Eq. 18 can be expressed as

$$B = yB_{AC} + (1-y)B_{AD} - y(1-y)B_{CD} \tag{19}$$

The interaction parameter B must be negative for a polymer blend to be miscible. Therefore, the miscibility of a blend containing a copolymer depends on the segmental B_{CD} values and the copolymer composition, as indicated in Eq. 19. As a result, the random copolymer segments that have strong segregation (i.e., a larger value of B_{CD}) would have better miscibility when blended with other homopolymers. Because PVPh and PS are immiscible, the value of B in Eq. 19 tends to be negative, while the value of B_{CD} is positive. The incorporation of styrene moieties into PVPh enhances the interactions of PVPh with PAS (rather than with PS) and, thus, improves their miscibility. The concept of a copolymer repulsion effect is consistent with the Painter–Coleman association model in this blend system.

Ternary polymer blends

In addition to incorporating styrene moieties (diluent segments) into PVPh main chains, we have reported that the addition of PEO also enhances the miscibility of immiscible PVPh/PAS binary blends at low PEO contents [109]. Figure 16 displays the C=O stretching region of the room-temperature IR spectra of pure PAS, a PAS/PVPh= 20/80 blend, and various PEO/PAS/PVPh ternary blends featuring a constant PAS/PVPh ratio (20/80).

For the binary PAS/PVPh blend, interestingly, the fraction of hydrogen-bonded C=O groups increased when the PEO content was 20 wt.%. The inter-association equilibrium constant of the PVPh/PAS blend (K_A=43.1) is smaller than the self-association equilibrium constant of pure PVPh (K_B=66.8), indicating that pure PVPh favors intra-chain hydrogen bonding. The addition of PEO into the PVPh/PAS blend decreases the strong self-association in the PVPh component because the inter-association equilibrium constant (K_A=88.3) [29] of PVPh with PEO is greater than the self-association equilibrium constant of pure PVPh. As a result, the fraction of hydrogen-bonded C=O groups of PAS increased at a PEO content at 20 wt.% because of the increased probability of OH-to-C=O hydrogen bonding. Therefore, the immiscible PAS/PVPh polymer blend transformed into a miscible blend after the

**Fig. 16** Infrared spectra recorded for ternary PEO/PAS/ PVPh blends
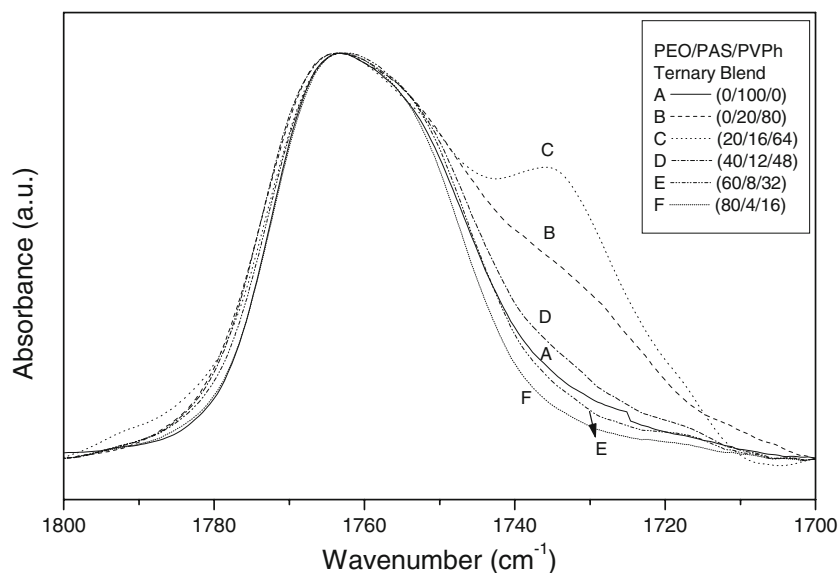
addition of a low content of PEO as a result of decreasing the degree of self-association of PVPh. The addition of PEO into PVPh/PAS binary blends constitutes the formation of a ternary blend system.

Multicomponent polymer blends are of significant industrial importance because their formation provides a convenient and attractive route toward new polymeric materials. Although increasing the number of polymer components in a polymer blend makes the system much more complicated, it does provide enhanced design flexibility for the control of multiple properties. There are several good reasons for studying ternary polymer blends: (1) As revealed by Scott [110] and Tompa [111], a polymer B that is miscible individually with polymers A and C can form miscible ternary polymer blends from immiscible binary pairs of A and C; i.e., polymer B acts as a "compatibilizer" that reduces the size domain of the heterogeneous phase separated structure. Classical examples of such systems are the ternary PVDF/PMMA/PEMA [112], PVPh/PMMA/PEMA [113], and SAN/PMMA/PEMA [114] blends. (2) The fabrication of totally miscible ternary polymer bends offers a unique opportunity to develop new polymer materials possessing properties arising from a flexible combination of those of its three components. (3) When all three binary pairs (B/A, B/C, and A/C) are individually miscible, completely homogeneous and closed immiscibility loop phase diagrams have been observed. The phase separation is caused by the difference in the interaction energy of the binary system, the so-called "$\Delta\chi$" and "ΔK" effects in ternary polymer blends [115, 116]. In this case, we can tune the phase behavior by controlling the composition in the ternary blend system.

In terms of the "comaptibilizer" effect, we have reported that the addition of BPA enhances the miscibility of PVAc/PVP immiscible binary blends, eventually transforming them into miscible blends possessing a single value of T_g when a sufficiently large amount of the BPA is present [117]. Figure 17a provides selected DSC curves (recorded during the second heating scan) of several BPA/PVAc/PVP ternary blends of various compositions. The PVAc/PVP binary polymer blend exhibits two glass transitions that are located at the same temperatures as those of their respective pure polymers, revealing that this binary blend is completely immiscible.

The values of T_g shift, however, with increasing BPA content; ultimately, the addition of a sufficiently large amount of BPA results in a miscible pair exhibiting a single value of T_g, because BPA forms hydrogen bonds with both PVAc and PVP. Figure 17b displays the phase diagram of the ternary BPA/PVAc/PVP blends, as determined from DSC analyses. The presence BPA enhances the miscibility of the PVAc/PVP binary blends, with the miscibility window shifting to the rich PVP region as a result of significant $\Delta\chi$ and ΔK effects.
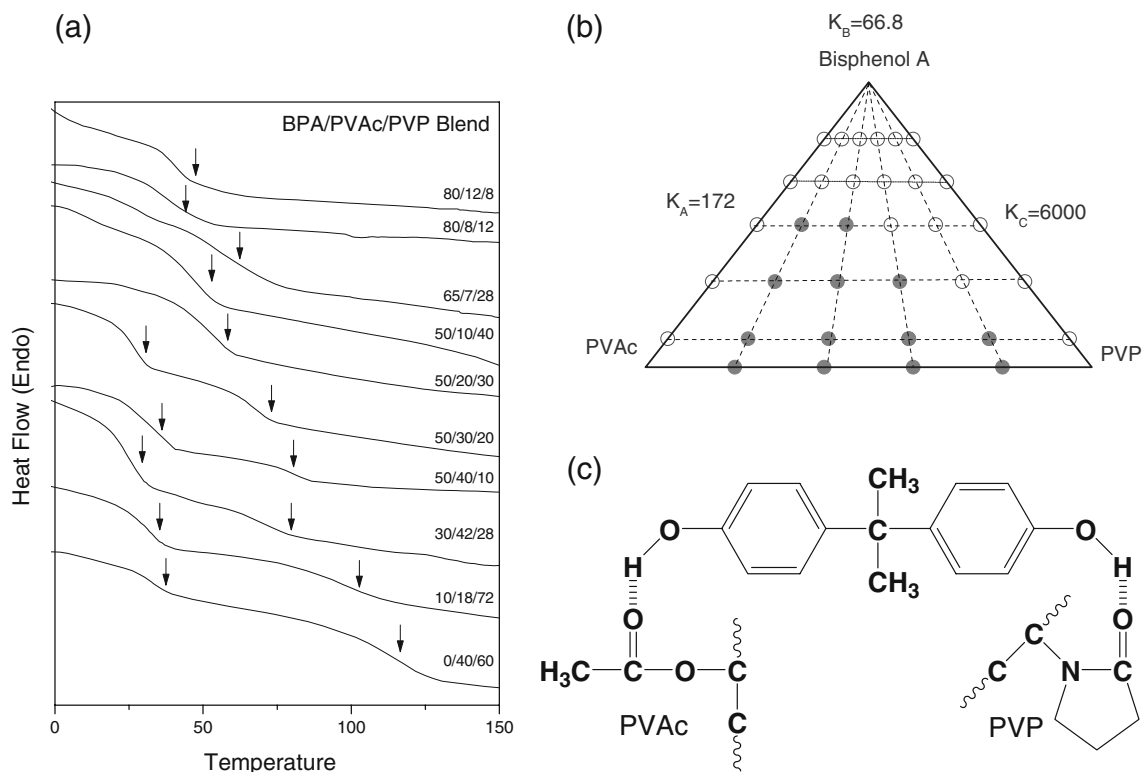
Fig. 17 a DSC thermograms of BPA/PVAc/PVP ternary blend, b ternary phase diagram, c hydrogen bonding interaction between BPA with PVAc and PVP

Similarly, we have also investigated the enhanced miscibility observed after the addition of BPA to immiscible PCL/PLLA binary biodegradable blends [118]. Although PLLA is studied and used widely because of its high biocompatibility and biodegradability [119, 120], its major disadvantage is the transition from ductile to brittle failure under tension as a result of its high melting temperature. In contrast, PCL possesses low glass transition and melting temperatures, and is added to PLLA in the role of a plasticizer to render it more flexible and to reduce its brittleness [121, 122]. Therefore, it is reasonable to expect that blending PLLA with PCL would either improve the flexibility or increased the strength with respect to the properties of the individual components. We have reported that bisphenol A—a low-molecular-weight, bifunctional hydrogen bond donor—interacts with both PCL and PLLA, which are both hydrogen bond-accepting polymers, to act as a compatibilizer that improves their miscibility [123–135].

In terms of studies into totally miscible ternary polymer bends that offer unique opportunities for developing new polymeric materials, only a very few ternary polymer blends have been reported that are homogeneous over their entire range of compositions. These totally miscible ternary blends—including PECH/PMMA/PEO [136], PVDF/PVAc/PMMA [137], PHB/PEO/PECH [138], PEDEK/PEEK/PEI [139], PEI/PET/PBT [140], and PCL/PPzMA/PBzMA [141]—all possess low $\Delta\chi$ effects and hydrogen bonding interactions between their polymer segments; i.e., the ΔK effect can be neglected. Coleman and Painter noted that only in very rare cases, such as the PVPh/PVAc/PMA

ternary blend [20], can completely miscible ternary polymer blends exist, because the $\Delta\chi$ and ΔK interactions must be finely balanced. The chemical structures of the PVAc and PMA repeat units are isomorphous and, thus, their ternary polymer blend displays a completely homogeneous amorphous phase. We were curious to answer the following question: Other than isomers of two polymers, is it possible to obtain totally miscible ternary polymer blends by taking advantage of hydrogen bonding? In our subsequent investigations, we discovered another completely miscible ternary hydrogen bonded polymer blend: that of phenoxy, phenolic, and PCL [142]. Figure 18 displays DSC thermograms of phenolic/phenoxy/PCL ternary blends of various compositions; each ternary blend exhibits only a single glass transition temperature, which strongly suggests that this ternary polymer blend is fully miscible over its total range of compositions.

In terms of studies of systems in which all three binary pairs (B/A, B/C, A/C) are individually miscible, completely homogeneous and closed immiscibility loop phase diagrams have been observed for such systems as phenoxy/PMMA/PEO [143], PVPh/PVAc/PEO [81], and SAA/PMMA/PEO [144]. We have also reported the phase behavior and hydrogen bonding present in ternary polymer blends of phenolic resin, PEO, and PCL [145].

Although all three binary blends are respectively miscible, there exists a closed immiscibility loop in the phase diagram because of the so-called "$\Delta\chi$" and "ΔK" effects in this hydrogen-bonded ternary polymer system. Figure 19a displays the second-run DSC thermograms of

Fig. 18 DSC thermograms of phenoxy/phenolic/PCL blends having different compositions
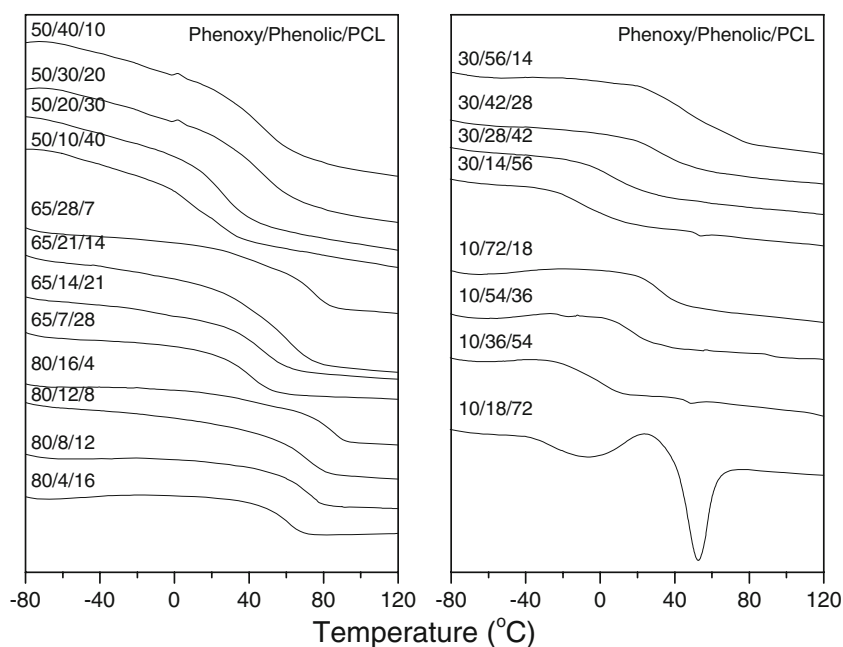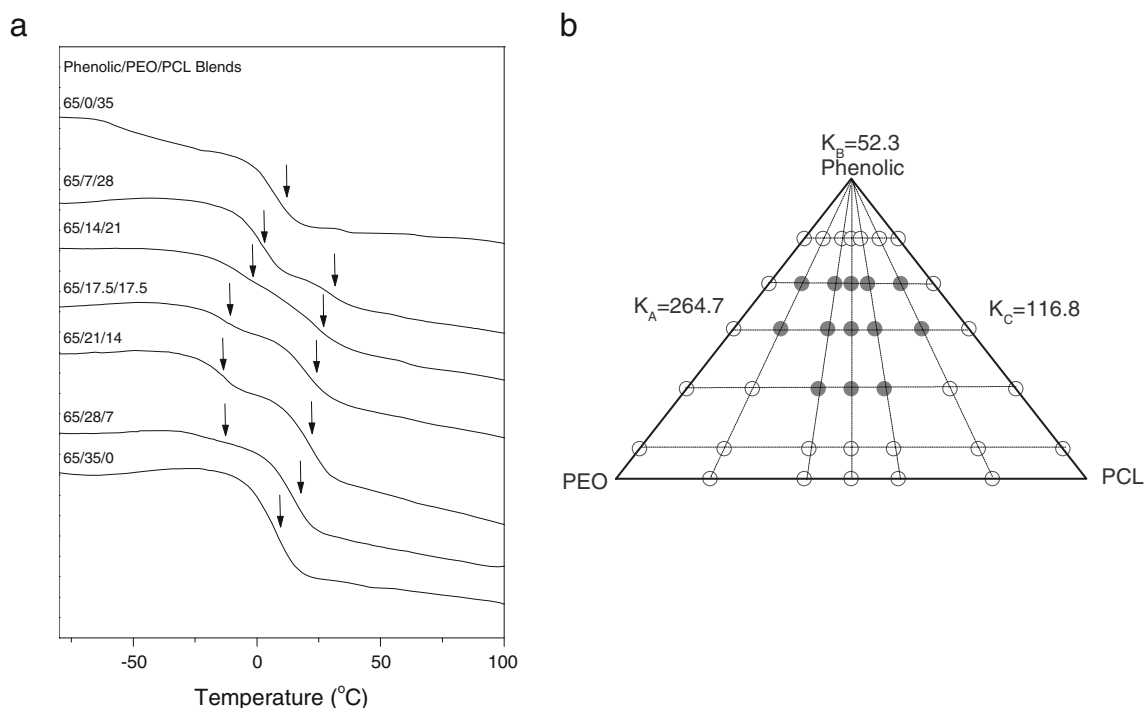
Fig. 19 **a** DSC thermograms of phenolic/PEO/PCL ternary blend, and **b** phase diagram of phenolic/PEO/PCL ternary blend

various phenolic/PEO/PCL ternary blends containing a constant phenolic content of 65 wt.%. The binary phenolic/PEO and phenolic/PCL blends each exhibit a single value of T_g, revealing that these binary blends are miscible in the amorphous phase. In contrast, the phenolic/PEO/PCL ternary blends containing 65 wt.% phenolic all display two glass transitions, implying that they are immiscible in the amorphous phase. In general, the phase separation in a ternary blend is caused by the so-called $\Delta\chi$ effect, which is the difference in the degrees of physical interaction between phenolic/PEO and phenolic/PCL. In addition, a difference in the inter-association equilibrium constant also tends to induce phase separation. Phenolic interacts more favorably with PEO than with PCL; such behavior is an example of the ΔK effect.

Figure 19b presents the phase diagram of the ternary phenolic/PEO/PCL blend at room temperature, based on DSC analyses. A closed-looped of the phase-separated region exists in the phase diagram, due to the so-called "$\Delta\chi$" and "ΔK" effects in the ternary polymer blend. Based on the behavior of this phenolic/PEO/PCL ternary blend, we applied this system to the preparation of a polymer electrolyte by replacing phenolic resin with lithium perchlorate (LiClO$_4$). We found that the miscibility of the LiClO$_4$/PEO/PCL ternary blend affects its ionic conductivity [146, 147]. Although individually these three binary blends are fully miscible, a closed immiscibility loop exists in their ternary blend phase diagram as a result of the existence of and competition between the complex interactions of the LiClO$_4$/

PEO, LiClO$_4$/PCL, and PEO/PCL pairs. Interestingly, we found that the maximum ionic conductivity (6.3×10^7 S cm^{-1}) at ambient temperature of the ternary blend at a fixed LiClO$_4$ content of 25 wt.% occurred at a composition of 25/60/15 (LiClO$_4$:PEO:PCL), which is close to the closed-loop region in the phase diagram [146].

Thermal properties of hydrogen-bonded polymers

In the following subsections, we discuss how hydrogen bonding has a significant effect on the thermal properties and crystallization behavior of polymer blends.

Glass transition temperature

The glass-transition temperature is an important intrinsic characteristic that influences the material properties of a polymer and its potential applications. Indeed, the most commonly used method for establishing the miscibility of several components is the detection of a single glass transition temperature. Over the years, a number of equations have been proposed to describe the relationship between T_g and composition of miscible polymer blends or copolymers, including the linear rule and the Fox [148], Gordon–Taylor [149], Couchman–Karasz [150–153], Kwei [154], and Braun–Kovacs [100] equations. Table 3 summarizes these equations for miscible blends.

Table 3 The composition dependence of the T_g of miscible blend

	Equations	Parameter
Linear rule	$T_g = W_1 T_{g1} + W_2 T_{g2}$	
Fox	$\frac{1}{T_g} = \frac{W_1}{T_{g1}} + \frac{W_2}{T_{g2}}$	
Gordon–Taylor	$T_g = \frac{W_1 T_{g1} + k W_2 T_{g2}}{W_1 + W_2}$	k: adjustable parameter
Couchman	$\ln T_g = \frac{W_1 \ln T_{g1} + k W_2 \ln T_{g2}}{W_1 + k W_2}$	k: adjustable parameter
Kwei	$T_g = \frac{W_1 T_{g1} + k W_2 T_{g2}}{W_1 + W_2} + q W_1 W_2$	k: adjustable parameter, q: interaction parameter term
Braun–Kovacs	$T_g = T_{g1} + \frac{\phi_2 f_{g2} + g \phi_1 \phi_2}{\phi_1 \Delta \alpha_1}$	g: interaction parameter term

where W_1 and W_2 denote weight fractions of the compositions, T_{g1} and T_{g2} represent the corresponding blend component glass transition temperatures, and k, q, and g are fitting constants. $\Delta \alpha_1$ is the difference between the volume expansion coefficients in the glassy and liquid state.

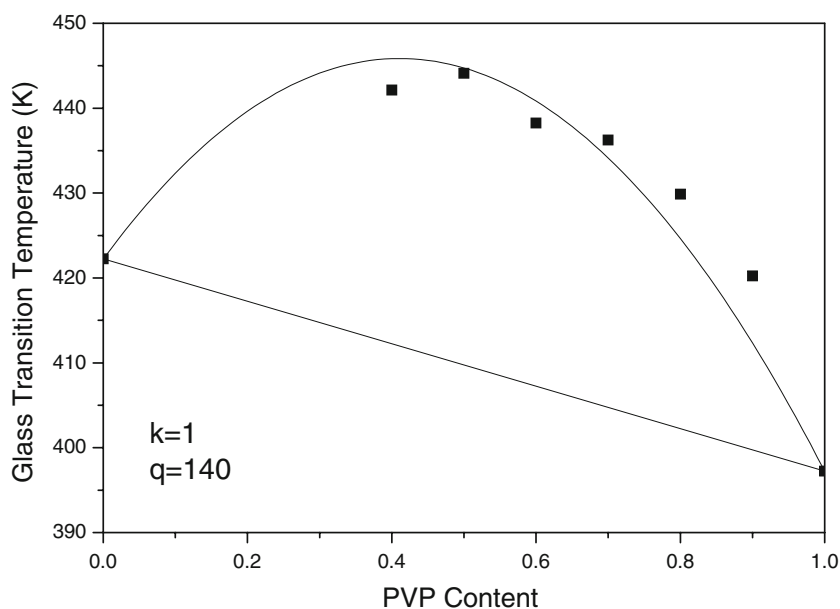## Positive deviation of glass transition temperature

Generally speaking, the presence of hydrogen bonds should raise the value of T_g because it restricts the motion of the polymer segments. Because the strong interactions between the components, the values of T_g observed for hydrogen-bonded blends—e.g., PVPh blended with PVP [43], P4VP [155], PMMA [156–158], poly(2-dimethylamino ethyl methacrylate) [159], poly(methyl piperidine–methyl methacrylate) [160], and poly(ethyleneimine) [161]—are usually higher than those predicted using the linear rule. Figure 20 displays the dependence of T_g on the composition of miscible PVPh/PVP blends; the maximum deviation on the

highest value of T_g was obtained when the blend composition was PVPh/PVP=50/50 [43].

In addition, values of k and q of 1 and 140, respectively, were obtained from the non-linear least-squares "best fit" of the values to the Kwei equation. Similar positive deviations of T_g have been observed for PHEMA/PVP [162], PHPMA/P4VP [163], phenolic/PVAc [164], phenolic/P4VP [165], phenolic/PVP [166], phenolic/PEOx [167], and polybenzoxazine/PVP [56] blends. Polymers possessing high glass-transition temperatures are attractive for industrial polymer science because of the strong economic rewards that would arise from their potential applications. For this reason, Coleman et al. [168] reported a copolymer that has a higher value of T_g than its corresponding polymer blend, because of higher composition heterogeneities in the hydrogen-bonded copolymer. According to the PCAM, the inter-association equilibrium constant of PVPh-co-PMMA (K_A=67.4) is higher than the inter-association equilibrium constant of the PVPh/PMMA blend (K_A=37.4), implying that the experimental values of T_g for copolymers and blends of the same composition should be different [169].

This result can be explained by considering the different degrees of rotational freedom arising from intramolecular screening and spacing effects. This phenomenon can also be interpreted in terms of the correlation hole effect described by de Gennus [170]. Accordingly, we synthesized a series of copolymers containing various vinylphenol and vinylpyrrolidone contents to compare their glass transition temperatures with those of corresponding PVPh/PVP blends [171, 172]. Figure 21 displays DSC traces revealing the thermal behavior of the corresponding PVPh-co-PVP copolymers. The observed glass transition temperatures increased in the order PVPh-co-PVP copolymer > PVPh/

Fig. 20 T_g versus composition curves: experimental data (*filled square*) and Kwei equation (*solid line*)

Fig. 21 DSC thermograms of PAS-*co*-PVP, pure PVP, PVPh/PVP and PVPh-*co*-PVP

(d) PVPh74-co-PVP26

(c) PVPh74/PVP26 Blend

(b) pure PVP
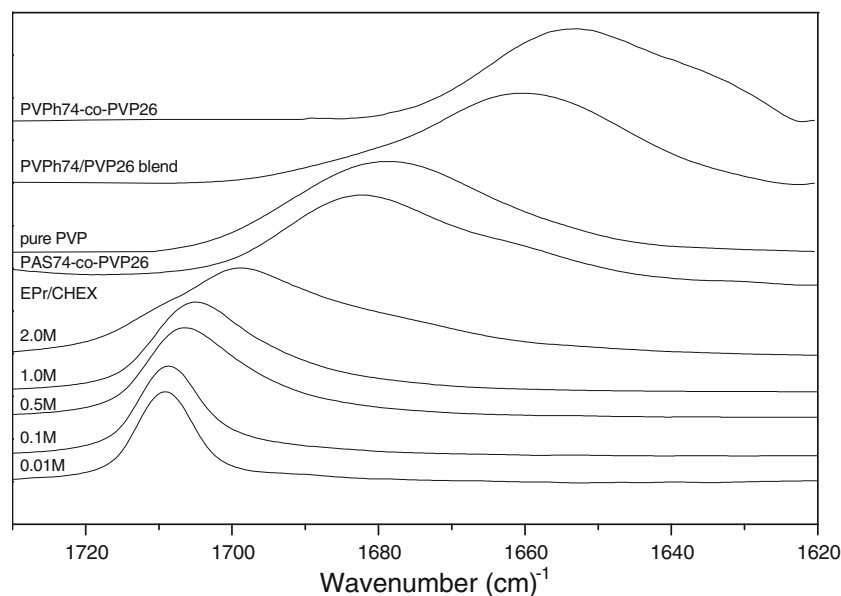
(a)PAS74-co-PVP26
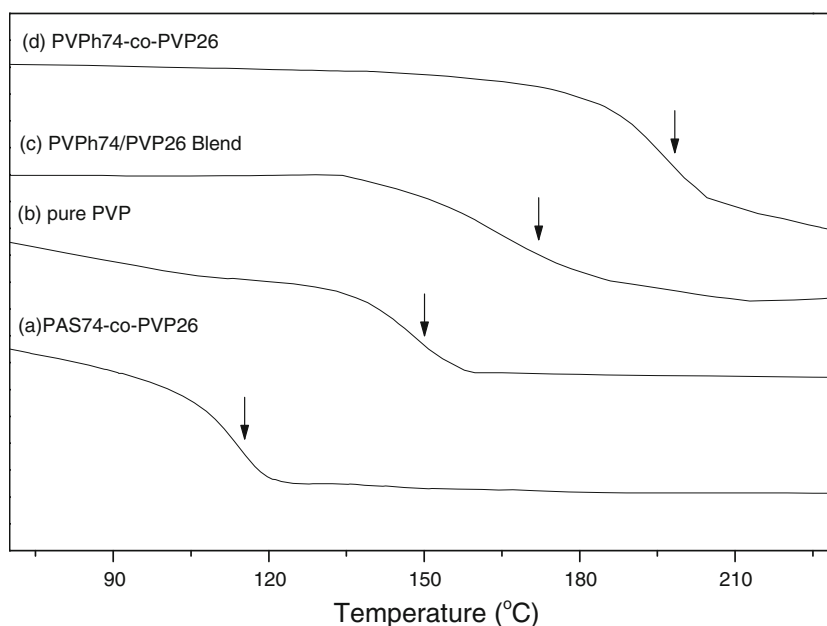
Temperature (°C)

PVP blend > pure PVP polymer > PAS-*co*-PVP copolymer. This significant increase in glass transition temperature prompted us to investigate the specific interactions that existed in these polymer systems at the same mole fraction of PVP.

Figure 22 displays the C=O stretching region in the corresponding FTIR spectra recorded at room temperature. [171]. The wavenumbers and half-widths of the signals in the IR spectra of polymers are affected dramatically by dipole–dipole or hydrogen bonding interactions with other molecules or polymer chains. The C=O band became broader and shifted to lower wavenumber upon increasing the concentration of ethyl pyrrolidone (EPr, a model compound for PVP) in CHEX—a result of the increased probability of pyrrolidone–pyrrolidone interactions.

The C=O signal for pure PVP occurs at a lower wavenumber and with a broader half-width relative to those of EPr in CHEX because no inert diluent (nonpolar group) is present in pure PVP and the probability of dipole–dipole interactions is presumably greater, as mentioned previously. The half-width of the signal for pure PVP at 1,680 cm^{-1} decreased and shifted to higher wavenumber

Fig. 22 FTIR spectra various EPr concentrations in cyclohexane, PAS-*co*-PVP copolymer, pure PVP, PVPh/PVP blend and PVPh-*co*-PVP copolymer

PVPh74-co-PVP26

PVPh74/PVP26 blend

pure PVP

PAS74-co-PVP26

EPr/CHEX

2.0M

1.0M

0.5M

0.1M

0.01M

Wavenumber (cm)$^{-1}$

(1,682 cm^{-1}) after incorporating acetoxystyrene monomer into the PVP chain (i.e., forming PAS-*co*-PVP). As a result, the value of T_g of the PAS-*co*-PVP copolymer decreased significantly relative to that of PVP because of the lower number of dipole–dipole interactions of the pyrrolidone moieties in the polymer chain. After deacetylation of PAS-*co*-PVP to form PVPh-*co*-PVP, however, the C=O absorption shifted from 1,680 to 1,651 cm^{-1}. This shift is attributed to the formation of hydrogen bonds between the vinylphenol and vinylpyrrolidone segments of the copolymer. In contrast, the same C=O stretching frequency for the PVPh/PVP blend shifts to only 1,660 cm^{-1}. This behavior suggests that the number (or strength) of hydrogen bonds within the PVPh-*co*-PVP copolymer is greater than that in the corresponding PVPh/PVP blend; this concept is consistent with the observed difference in glass transition temperatures between the PVPh-*co*-PVP copolymer and the PVPh/PVP blend.

Similar to the PVPh/PVP system, we also investigated the increase in T_g of PMMA copolymers arising through hydrogen bonding interactions [173–175]. PMMA is a transparent polymeric material possessing many desirable properties, such as light weight, high light transmittance, chemical resistance, colorlessness, resistance to weathering corrosion, and good insulating properties [176]. The glass transition temperature of PMMA, however, is relatively low (ca. 100 °C), which limits its applications in the optics and electronics industries—for materials such as compact discs (CDs), optical glasses, and optical fibers—because it undergoes distortion when used in an inner glazing material [177, 178]. To raise PMMA's value of T_g, we investigated its copolymerization with methacrylamide (MAAM), taking advantage of the strong hydrogen bonding interactions that occur between these two monomer segments [179, 180].

The most well known of the commercialized miscible blend systems is that of poly(2,6-dimethyl-1,4-phenylene oxide) (PPO) and PS, which has widespread commercial application in the thermoplastics industry [181–183]. The dependence of the value of T_g on the composition of miscible PPO/PS blends obeys the Fox rule. Because we knew that the values of T_g of copolymers are substantially higher than those of the corresponding blend systems, we attempted to raise the value of T_g of the miscible PPO/PS blend by synthesizing the PPO-*b*-PS copolymer through atom transfer radical polymerization [184]. It is worth noting that the value of T_g of the PPO-*b*-PS copolymer having a PS content of 70 wt.% is approximately the same as that of the PPO/PS=50/50 blend. Thus, at an identical value of T_g, the PPO-*b*-PS copolymer is cheaper (in terms of having a lower PPO content) and easier to process (higher PS content) than the PPO/PS blend. We have also reported several systems for which the glass transition temperature increases as a result of hydrogen bonding, including the PHEMA-*b*-PVP [185], PVPh-*co*-PMMA [186], PVPh-*b*-PCL [187], and PVPh-*b*-P4VP [51].

Negative deviation of glass transition temperature

Based on the experimental results, the increase in T_g does not always appear as a positive deviation from the weight-average law. For example, Fig. 23 reveals that the values of T_g for phenolic/PAS display a negative deviation from this law. In this case, the negative deviation indicates that the intermolecular hydrogen bonds were weaker than the intramolecular ones [63]. The observed reduction in T_g in these phenolic/PAS blends is caused by a partial decrease in the degree of self-association through intramolecular hydrogen bonding.

Fig. 23 T_g versus composition curves of phenolic/PAS blend
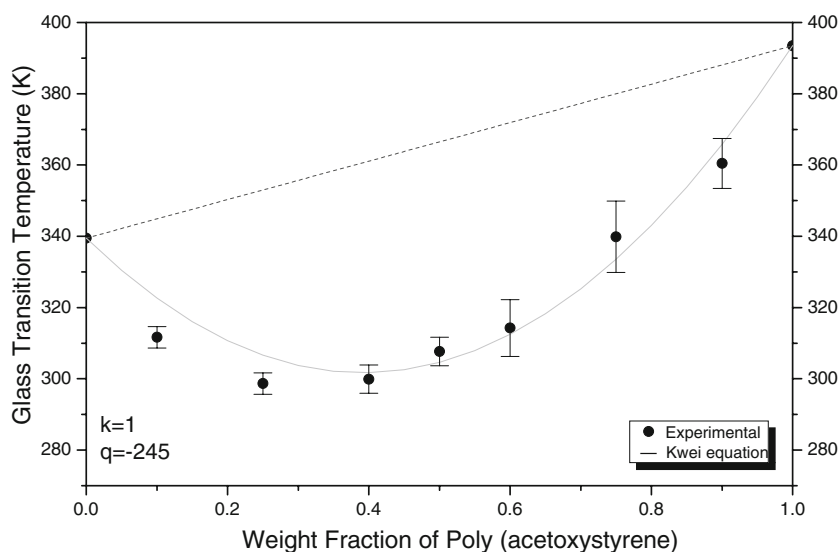
Similar negative deviations have been observed also in phenolic/PCL [64], PVPh/PCL [188], phenoxy/PCL [188], PVPh/phenoxy [189], phenolic/PMMA [190], PAS/PEO [191], and PVPh/PAA [192] blend systems. A strong negative deviation in the value of T_g of a polymer blend is a useful property for a polymer electrolyte [193–195]. Nevertheless, the question remains as to why both positive and negative deviations in T_g occur for systems featuring intermolecular hydrogen bonding.
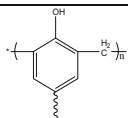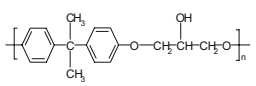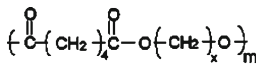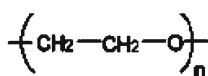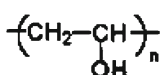
Wu et al. proposed an excellent rationale to explain these discrepancies [196]; they examined the behavior of four different hydrogen bond acceptors (modifiers)—phenoxy, PDA, PEO, and PVA—the chemical structures and inter-association equilibrium constants of which are summarized in Table 4. The phenolic resin blended with a modifier having a longer repeating unit (e.g., phenoxy or PDA) exhibited a substantially negative deviation in T_g in the phenolic-rich region. In contrast, the phenolic resin blended with a modifier having the shorter repeating unit (e.g., PEO or PVA) displayed a positive deviation in the value of T_g. Similar to the variation of the content of "free" OH groups detected by IR spectroscopy, the deviation in T_g also differs for the various phenolic/modifier blends.

Because the values of K_A of these phenolic/modifier blends are substantially greater than those for self-association, these modifier chains presumably are able to extend as far as possible in these phenolic blends. According to the PCAM argument, the deviation in T_g is a result of an entropy change corresponding to the variation in the number of hydrogen bonding interactions within these phenolic blends. In the phenolic/PEO and phenolic/PVA blends, the PVA and PEO units possess short repeating units that contain higher densities of potentially hydrogen bonding functional groups and higher values of K_A; thus, they tend to form a higher density of intermolecular hydrogen bonds with phenolic. This phenomenon not only overcomes the energy of self-association upon blending but also reduces the entropy of the phenolic blend.

As a result, the frameworks of these blends become stiffer; thus, the observed positive deviations in T_g are expected. These two cases are similar to the results reported by in their original publications using PCAM [197–201]. In contrast, phenoxy and PDA molecules having long repeating units provide a relatively smaller number of potential hydrogen bonding sites and, hence, form fewer intermolecular hydrogen bonds with phenolic. For modifiers having long repeating units, the reduction in entropy upon forming a phenolic–modifier interaction is not sufficiently high to overcome the entropy increase associated with disrupting the self-association of phenolic. A long repeating unit length and a low density of potential hydrogen bonding sites induces an additional entropy factor, $-T\Delta S_m$, which elevates the entropy upon blending and, thus, results in a substantial reduction in the value of T_g of these phenolic

Table 4 Self-and inter association equilibrium constant between phenolic and modifiers [187]

Material	Molecular structure	Self-association constant		Inter-association constant
		K_2	K_B	K_A
Phenolic resin		23.3[a]	52.3[a]	
Phenoxy		14.4[a]	25.6[a]	114.0
Poly(adipic ester)				89.5
Poly(ethylene oxide)				67.6
Poly(vinyl alcohol)		26.7	44.1	121.8

blends. The variation in $-T\Delta S_m$ of phenolic/modifier blends incorporating long repeating units is greater (further away from zero) than that of phenolic/modifier blends featuring short repeating units.

Melting temperature

The depression of the melting point of a crystalline polymer blended with an amorphous polymer provides important information about its miscibility and its associated polymer–polymer interaction parameter. The reduction in melting temperature is caused by both morphological and thermodynamic effects. The thermodynamic properties of the crystalline component in the amorphous phase can be determined. When two polymers are miscible in the molten state, the chemical potential of the crystallizable polymer decreases as a result of the addition of the second component. This phenomenon leads to a reduction in the equilibrium melting temperature of the resulting blend. The data obtained in this study were analyzed using the Nishi–Wang equation [202] based on the Flory–Huggins theory [52]. The melting point depression is given by Eq. 20:

$$\frac{1}{T_m^0} - \frac{1}{T_{m2}^0} =$$
$$\frac{-R}{\Delta H_{2u}} \frac{V_{2u}}{V_{1u}} \left[\frac{\ln \phi_2}{x_2} + \left(\frac{1}{x_2} - \frac{1}{x_1} \right)(1 - \phi_2) + \chi_{12}(1 - \phi_2)^2 \right]$$
$$(20)$$

where T_m^0 and T_{m2}^0 denote the equilibrium melting points of the pure crystallizable component and the blend, respectively; V_{2u} and V_{1u} are the molar volumes of the repeating units of the polymers; R is the universal gas constant; ΔH_{2u} is the heat of fusion of the perfectly crystallizable polymer per mole of repeat unit; the subscripts 1 and 2 represent the amorphous polymer and the crystalline polymer, respectively; x_1 and x_2 are the degrees of polymerization; Φ is the volume fraction of the component in the blend; and χ_{12} is the polymer–polymer interaction parameter. When both x_1 and x_2 are large, for high-molecular-weight polymers, these related terms in Eq. 20 can be neglected. The interaction parameter χ_{12} can be written as

$$\chi_{12} = \frac{BV_{1u}}{RT} \qquad (21)$$

Substituting Eq. 3 into Eq. 2 yields the Nishi–Wang equation (22):

$$T_m^0 - T_{m2}^0 = -T_m^0 \frac{BV_{2u}}{\Delta H_{2u}} \phi_1^2 \qquad (22)$$

where $\Delta H_{2u}/V_{2u}$ is the latent heat of fusion of the 100% crystalline component per unit volume and B denotes the interaction energy density between the blend components.

In addition, Painter and Coleman modified the Nishi–Wang equation to account for hydrogen bonding, simply by considering the value of ΔG_H as part of the partial molar free energy [20]:

$$\frac{1}{T_m} - \frac{1}{T_m^0} = -\frac{R}{\Delta H_f^0} \left[\Phi_B^2 \chi + \Delta G_H \right] \qquad (23)$$

Almost all hydrogen-bonded polymer blend systems exhibit significant melting point depressions—because of the contribution from ΔG_H—if the blends contain a semicrystalline component. Therefore, different hydrogen bonding strengths induce different melting point depressions.

Crystallization behavior

Crystalline polymers are ubiquitous, ranging from commodities (e.g., polyethylene) to high-performance engineering resins (e.g., nylons and PEEK). Many authors have discussed the crystallization behavior of polyethylene [203–207], for which no specific interactions occur within its main chains. Therefore, there is quite a lot of interest in studying crystallization in polymer blends with regard to intermolecular interactions, such as hydrogen bonding and dipole–dipole interactions. Relative to neat crystalline materials, the crystalline microstructures and crystallization kinetics of polymer blends containing crystalline polymers are less well understood because of their inherent complexities. As a result, it is necessary to establish general principles to predict the nature of polymer crystallization in polymer blends.

Generally, the growth kinetics of a crystallizable component are depressed upon the addition of an amorphous component because of (1) the reduction of chain mobility, (2) the dilution of the crystallizable component at the growth front, (3) the change in free energy of nucleation as a result of specific interactions, and (4) the morphology of the amorphous/crystallization binary blend that results in competition between the advancing spherulite front and diffusion of the amorphous component into the interlamellar and interfibrillar region. Other parameters—namely the crystallization kinetics, the surface free energy of chain folding, and the thickness of the crystalline phase in miscible polymer blends formed through hydrogen bonding—have received relatively less attention [208, 209]. In general, the crystallization kinetics and microstructures of a crystalline blend depend on the various effects of the glass transition temperature and degree of intermolecular interactions of the diluent amorphous phase. Runt et al. [208] found that blends of PEO with amorphous polymeric diluents exhibited either relatively weak interactions (e.g., PVAc and PMMA) or strong hydrogen bonding interactions [e.g., ethylene-co-methacrylic acid55 (EMAA55, 55 wt.% MAA) copolymer and styrene-co-hydroxystyr-

ene50 (SHS50, 50 wt.% hydroxystyrene) copolymer]. At a given crystallization temperature (T_c), the spherulite growth rates for blends containing strongly hydrogen bonding polymers are considerably lower than those featuring weakly interacting polymers having comparable glass transition temperatures; cf. the PMMA/PEO and SHS/PEO or the PVAc/PEO and EMAA/PEO blend systems. Furthermore, a study of the spherulite radius of PEO in blends with the strongly interacting EMAA55 and SHS50 revealed that the SHS50/PEO blend had slower crystallization kinetics than did the EMAA50/PEO blend because of the higher glass transition temperature of SHS; the different intermolecular hydrogen bonding strengths in the SHS/PEO and EMAA/PEO blends were not, however, considered. Therefore, we have proposed a general principle to rationalize the crystallization kinetics, surface free energies of chain folding, and crystal thicknesses with respect to the various strengths of hydrogen bonds present in crystalline polymer blends.

We studied the hydrogen bonding strengths in PCL blends of three different well-known hydrogen bond-donating polymers: phenolic, PVPh, and phenoxy. Cortazar et al. studied the crystallization kinetics and melting behavior of the phenoxy/PCL blend and found that the surface free energy of chain folding of the PCL blend with phenoxy was lower than that of pure PCL [210]. The same trend was also observed in PVC/PCL [121] and SAN/PCL [211] blend systems. We found, however, that the surface free energy of chain folding increases upon increasing the phenolic content. According to the secondary nucleation theory [212], the initial crystal thickness is dependent not only on the degree of supercooling but also on the value of the surface free energy of chain folding. As a result,

determining the surface free energy of chain folding is quite important because the morphology of a crystalline PCL blend depends strongly on this value. These trends indicate that different hydrogen bonding strengths can affect a polymer's crystallization in terms of its thermodynamic properties and morphology.

Table 5 lists the K_A/K_B ratios and corresponding surface free energies of chain folding for various hydrogen-bonded crystalline polymer blends [77].

Clearly, if the inter-association equilibrium constant is larger than the self-association equilibrium constant, the surface free energy in the polymer blend is larger than that in the pure crystalline homopolymer, as is the case for phenolic/PCL, PVPh/PCL, and phenolic/PEO blend systems [213]. Conversely, if the self-association equilibrium constant is greater than the inter-association equilibrium constant, the surface free energy in the polymer blend is smaller than that in the pure crystalline homopolymer, as is the cases for phenoxy/PCL and PVPh/PHB [214] blend systems. In addition, the surface free energy in a polymer blend featuring a relatively weaker interaction is smaller than that in the pure crystalline homopolymer, as is the case for PVC/PCL, SAN/PCL, and PMA/PHB [215].

Although the crystallization kinetics decrease upon increasing the amount of the amorphous component in all of these miscible blend systems, the surface free energies of chain folding exhibit various trends with different intermolecular interaction strengths. In a blend systems featuring strong hydrogen bonding, the surface free energy of chain folding increases upon increasing the content of phenolic or PVPh. This phenomenon is probably related to the fact that phenolic and PVPh easily form entanglements or physical crosslinks with PCL molecules during crystallization,

Table 5 The relationship between the relative magnitude strength of K_A versus K_B with surface free energy of chain folding and crystal layer thickness [77, 223]

Blend System	K_A	K_B	K_A/K_B	σ_e	l_c
Strongly hydrogen bonding					
Phenolic/PCL	116.8	52.3	$K_A>K_B$	Increase	Increase
PVPh/PCL	90.1	66.8	$K_A>K_B$	Increase	Increase
Phenolic/PEO	264.7	52.3	$K_A>K_B$	Increase	–
SHS50/PEO	88.3	33.4	$K_A>K_B$	–	Increase
Weakly hydrogen bonding					
Phenoxy/PCL	7.0	25.6	$K_A<K_B$	Decrease	Decrease
PVPh/PLLA	10	66.8	$K_A<K_B$	–	Decrease
PVPh/PHB	62.1	66.8	$K_A<K_B$	Decrease	Decrease
ACA/PHB	2.6	28.8	$K_A<K_B$	Decrease	Decrease
Weakly interaction					
PVC/PCL				Decrease	Decrease
SAN/PCL				Decrease	Decrease
PMA/PHB				Decrease	–
PVAc/PHB				–	Increase
PVAc/PEO				–	Increase

which favors the formation of large loops on the surfaces of lamellar PCL crystals.

These results indicate that the surface enthalpy term overwhelms the surface entropy of chain folding when K_A is greater than K_B. In contrast, in a system featuring weak hydrogen bonding—e.g., for phenoxy acting as a nucleation agent for PCL, where K_B is greater than K_A—the blend tends to be immiscible or partially miscible and, thus, there is a decrease in the free energy change upon crystallization, which is the driving force for crystallization. The same concept has been used to explain the behavior of relatively weakly interacting blends, such as the SAN/PCL blend [202]. A recent theoretical model has predicted that a miscible blend of polymers having a relatively large difference in their values of T_g and exhibiting weak intermolecular interactions will exhibit "two dynamic microenvironments" [216]: one near the mean blend mobility and the other close to that of the component having the lower value of T_g. Nevertheless, DSC analyses of weakly hydrogen bonding blends (e.g., phenoxy/PCL) and weakly interacting blends (e.g., PVC/PCL or SAN/ PCL) reveal only single values of T_g.

It is generally established that a single compositionally dependent glass transition indicates full miscibility with dimensions on the order of 20–40 nm, but no lower. For example, DSC analyses of the well-known hydrogen-bonded blend system PVPh/PMMA reveal only a single value of T_g. Two dynamic relaxations are found, however, in analyses performed using a dynamic mechanical analyzer and observing the spin lattice relaxation time in the rotating frame [$T_{1\rho}$(H)] in solid state NMR spectroscopy [217–219], because the value of K_A between the OH group of PVPh and the C=O group of PMMA (K_A=37.5) [165] is smaller than the value of K_B for the hydroxyl–hydroxyl interactions of PVPh (K_B=66.8). Two relaxation times in the rotating frame indicate that the immiscibility domain size is greater than 2–3 nm, based on the one-dimension spin-diffusion equation [220–222]. Therefore, micro-phase separation might occur in certain relative weakly hydrogen bonding or weakly interacting blend systems, indicating that the amorphous component can play the role of a nucleation agent to reduce the surface free energy of chain folding and provide the driving force for crystallization. As a result, different values of surface free energy of chain folding tend to induce different crystal layer thicknesses, which is dependent on the competition between the surface free energy of chain folding and the degree of supercooling.

Conclusions

This Review summarizes the recent results of studies of hydrogen bonds within polymer blends. Clearly, several factors influence the formation of hydrogen bonds, such as the solvents used, intramolecular screening effects, functional group accessibility, the acidities of the hydrogen bond donors, the basicities of the hydrogen bond acceptors, steric hindrance, the bulk of the side groups, and the temperature. Each of these factors also affects the ratio of the inter-association and self-association equilibrium constants.

The miscibility of polymer blends can be enhanced through hydrogen bonding after (a) incorporating functional groups into the main chain, (b) adding a third component into the immiscible binary blend, and (c) introducing an inert diluent segment into a strongly self-associating hydrogen bonding donor group. These methods are also effective for improving the compatibility and properties of immiscible blends.

The presence of hydrogen bonds significantly affects the thermal properties of polymers blends. Both positive and negative deviations from linearity have been observed for the glass transition temperatures of polymer blends featuring various types of repeat units. Furthermore, hydrogen-bonded copolymers exhibit higher values of T_g than do their corresponding polymer blends because of their higher composition heterogeneities. For a crystalline polymer, the melting temperature usually decreases upon increasing the content of the second hydrogen-bonding component. The crystal thickness is also dependent on the ratio between the inter-association and self-association equilibrium constants; a higher inter-association equilibrium constant enhances the surface energy of chain folding and, thus, increases the crystal thickness.

References

1. Boreo M, Ikeshoji T, Liew CC, Terakura K, Parrinello M (2004) J Am Chem Soc 126:6280
2. Murata T, Morita Y, Yakiyama Y, Fukui K, Yarnochi H, Saito G, Nakasuji K (2007) J Am Chem Soc 129:10837
3. Smith JD, Cappa CD, Wilson KR, Messer BM, Cohen RC, Saykally RJ (2004) Science 306:851
4. Jones WD (2000) Science 287:1942
5. Deechongkit S, Naguen H, Powers ET, Dawson PE, Gruebele M, Kelly JW (2004) Nature 430:101
6. Mehta R, Dadmun MD (2006) Macromolecules 39:8799
7. Fecko CJ, Eaves JD, Loparo JJ, Tokmakoff A, Geissler PL (2003) Science 301:1698
8. Watson FP, Crick FH (1953) Nature 171:964
9. Pauling L, Corey RB, Branson HR (1951) Proc Natl Acad Sci 37:205
10. Pauling L, Corey RB (1951) Proc Natl Acad Sci 37:729
11. Paul DR (1978) In: Paul DR, Newman S (eds) Polymer blends. Academic, New York
12. Utracki LA (1989) Polymer alloys and blends. Hanser, Munich

13. Coleman MM, Pehlert GJ, Yang X, Stallman JB, Painter PC (1996) Polymer 37:4753
14. Wang J, Cheung MK, Mi Y (2001) Polymer 42:2077
15. Li X, Goh SH, Lai YH, Wee ATS (2000) Polymer 41:6563
16. Sawateri C, Kondo T (1999) Macromolecules 32:1949
17. Cesteros LC, Isasi JR, Katime I (1993) Macromolecules 26:7256
18. Ma CCM, Wu HD, Lee CT (1998) Polymer 36:1721
19. Cassu SN, Felisberti MI (1999) Polymer 40:4845
20. Coleman MM, Painter PC (1995) Prog Polym Sci 20:1
21. Jiang M, Mei L, Xiang M, Zhou H (1999) Adv Polym Sci 146:121
22. He Y, Zhu B, Inoue Y (2004) Prog Polym Sci 29:1021
23. Binder WH, Zirbs R (2007) Adv Polym Sci 207:1
24. Bouteiller L (2007) Adv Polym Sci 207:79
25. Ten Brinke G, Ruokolaine J, Ikkala O (2007) Adv Polym Sci 207:113
26. Xu H, Srivastava S, Rotello VM (2007) Adv Polym Sci 207:179
27. Jeffrey GA, Saenger W (1991) Hydrogen bonding in biological structures. Springer, Berlin
28. Calhorda MJ (2000) Chem Commun 10:801
29. Coleman MM, Gref JF, Painter PC (1991) Specific interactions and the miscibility of polymer blends. Technomic, Lancaster, PA
30. Goh SH, Lee SY, Zhou X, Tan KL (1999) Macromolecules 32:942
31. Goh SH, Lee SY, Zhou X, Tan KL (1998) Macromolecules 31:4260
32. Jiao H, Goh SH, Valiyaveettil S (2001) Macromolecules 34:7162
33. Li L, Chan CM, Weng LT, Xiang ML, Jiang JM (1998) Macromolecules 31:7248
34. Weng LT, Chan CM (2000) Review Chemical Engineering 16:341
35. Zeng XM, Chan CM, Weng LT, Li L (2000) Polymer 41:8321
36. Goh SH, Lee SY, Yeo YT, Zhou X, Tan KL (1999) Macromol Rapid Commun 20:148
37. Yi JZ, Goh SH, Wee ATS (2001) Macromolecules 34:4662
38. Goh SH, Lee SY, Luo XF, Wong MW, Tan KL (2001) Macromol Chem Phys 202:31
39. Witter R, Sternberg U, Hesse S, Kondo T, Koch FT, Ulrich AS (2006) Macromolecules 39:6125
40. Kadla JF, Kubo S (2003) Macromolecules 36:7803
41. Xu JW, He CB, Toh KC, Lu XH (2002) Macromolecules 35:8846
42. Rachocki A, Tritt-Goc J (2006) J Polym Res 13:201
43. Kuo SW, Chang FC (2001) Macromolecules 34:5224
44. Kuo SW, Chang FC (2001) Macromolecules 34:4089
45. Dybowski C, Bai S, Bramer SV (2002) Anal Chem 74:2713
46. Lau C, Mi Y (2001) Polymer 43:823
47. Senake-Perara MC, Ishiaku US, Ishak ZAM (2001) Eur Polym J 37:167
48. Kesling B, Hughes E, Gullion T (2000) Solid State Nucl Magn Reson 16:1
49. Wu HD, Ma CCM, Chang FC (2000) Macromol Chem Phys 201:1121
50. Torres MAPR, Oliveira CMF, Tavares MIB (2000) Int J Polym Mater 46:695
51. Kuo SW, Tung PH, Chang FC (2006) Macromolecules 39:9388
52. Flory PJ (1953) Principles of polymer chemistry. Cornell University Press, Ithaca, NY
53. Sanchez IC, Stone MT (2000) In: Paul DR, Bucknall CB (eds) Polymer blend. Wiley, New York
54. Paul DR, Merfeld GD (2000) In: Paul DR, Bucknall CB (eds) Polymer blend. Wiley, New York
55. Coleman MM, Painter PC (2000) In: Paul DR, Bucknall CB (eds) Polymer blend. Wiley, New York
56. Su IC, Kuo SW, Yeh DR, Xu H, Chang FC (2003) Polymer 44:2187
57. Hu Y, Painter PC, Coleman MM (2000) Macromol Chem Phys 201:470
58. Ma CCM, Wu HD, Peter PC, Han TT (1997) Macromolecules 30:5443
59. Espi E, Iruin JJ (1991) Macromolecules 24:6456
60. Coleman MM, Yang X, Zhang H, Painter PC (1993) J Macromol Sci, Phys B32:295
61. Whestel KB, Lady JH (1970) Spectroscopy of fuels. Plenum, London
62. Coggesthall ND, Saier EL (1951) J Am Chem Soc 71:5414
63. Kuo SW, Chang FC (2002) Macromol Chem Phys 203:868
64. Kuo SW, Chang FC (2001) Macromol Chem Phys 202:3112
65. Painter PC, Veytsman B, Kumar S, Shenoy S, Graf JF, Xu Y, Coleman MM (1997) Macromolecules 30:932
66. Coleman MM, Pehlert GJ, Painter PC (1996) Macromolecules 29:6820
67. Pehlert GJ, Painter PC, Veytsman B, Coleman MM (1997) Macromolecules 30:3671
68. Pehlert GJ, Painter PC, Coleman MM (1998) Macromolecules 31:8423
69. Coleman MM, Guigley KS, Painter PC (1999) Macromol Chem Phys 200:1167
70. Pruthtikul R, Coleman MM, Painter PC, Tan NB (2001) J Polym Sci Polym Phys Ed 39:1651
71. Coleman MM, Painter PC (1998) Macromol Chem Phys 199:1307
72. Hu YH, Painter PC, Coleman MM, Butera RJ (1998) Macromolecules 31:3394
73. Coleman MM, Narvett LA, Park YH, Painter PC (1999) J Macromol Sci Phys B37:283
74. Painter PC, Berg LP, Veytsman B, Coleman MM (1998) Macromolecules 30:7529
75. Coleman MM, Painter PC (2006) Miscible polymer blends: background and guide for calculations and design. DEStech, Lancaster, PA
76. Kuo SW, Chang FC (2002) J Polym Sci Polym Phys Ed 40:1661
77. Kuo SW, Chan SC, Chang FC (2003) Macromolecules 36:6653
78. Han YK, Pearce EM, Kwei TK (2000) Macromolecules 33:1321
79. Zhao JQ, Pearce EM, Kwei TK (1997) Macromolecules 30:7119
80. Hu Y, Motzer HR, Etxeberria AM, Fernadez-Berridi MJ, Iruin JJ, Painter PC, Coleman MM (2000) Macromol Chem Phys 201:705
81. Manestrel CL, Bhagwagar DE, Painter PC, Coleman MM, Graf JF (1992) Macromolecules 25:7101
82. Irionod P, Iruin JJ, Fernandex-Berridi MJ (1996) Macromolecules 29:5605
83. Zhang LL, Goh SH, Lee SY (1998) J Appl Polym Sci 70:1811
84. Dai J, Goh SH, Lee SY, Siow KS (1996) Polymer 37:3259
85. Kuo SW, Lin CL, Chang FC (2002) Polymer 43:3943
86. Kuo SW, Wu CH, Chang FC (2004) Macromolecules 37:192
87. Coleman MM, Narvett LA, Painter PC (1998) Polymer 39:5867
88. Zhu B, Li J, He Y, Osanai Y, Matsumura S, Inoue Y (2003) Green Chem 5:580
89. Dong J, Ozaki Y (1997) Macromolecules 30:286
90. Cowie JMG, Reid VMC, McEwen IJK (1990) Polymer 31:486
91. Kressler J, Kammer HW, Schmidt-Naake G, Herzog K (1988) Polymer 29:686
92. Nishimoto M, Takami Y, Tohara A, Kasahara H (1995) Polymer 36:1441
93. Shimomai K, Higashida N, Ougizawa T, Inoue T, Rudolf B, Kressler J (1996) Polymer 37:5877
94. Paul DR, Barlow JW (1984) Polymer 25:4870
95. Panayiotou C (1987) Makromole Chemie 188:2733
96. Kanbour RP, Bendler JT, Bopp RC (1983) Macromolecules 16:753
97. Chien YY, Perace EM, Kwei TK (1988) Macromolecules 21:616

98. Kuo SW, Chang FC (2001) Polymer 42:9843
99. Kuo SW, Chang FC (2001) Macromolecules 34:7737
100. Kovacs A (1963) Adv Polym Sci 3:394
101. de Mefathi MV, Frechet JMJ (1988) Polymer 29:477
102. Prinos A, Dompros A, Panayiotou C (1998) Polymer 39:3011
103. Zhu KJ, Wang LQ, Yang SL (1994) Macromol Chem Phys 195:1965
104. Zhuang HF, Pearce EM, Kwei TK (1994) Macromolecules 27:6398
105. Park P, Zimmerman SC, Nakashima S (2005) J Am Chem Soc 127:6520
106. Park P, Zimmerman SC (2006) J Am Chem Soc 128:11582
107. Mugica A, Calahorra ME, Cortazar M (2002) Macromol Chem Phys 203:1088
108. Li G, Cowie JMG, Arrighi V (1999) J Appl Polym Sci 74:639
109. Kuo SW, Liu WP, Chang FC (2005) Macromol Chem Phys 206:2307
110. Scott RL (1949) J Chem Phys 17:279
111. Tompa H (1949) Trans Faraday Soc 45:1140
112. Kwei TK, Frisch HL, Radigan W, Vogel S (1977) Macromolecules 10:157
113. Pomposo JA, Cortazar M, Calahorra E (1994) Macromolecules 27:252
114. Goh SH, Siow KS (1986) Thermochim Acta 105:191
115. Patterson D (1982) Polym Eng Sci 22:64
116. Zhang H, Bhagwagar DE, Graf JF, Painter PC, Coleman MM (1994) Polymer 35:5379
117. Kuo SW, Chan SC, Chang FC (2002) Polymer 43:3653
118. Kuo SW, Huang CF, Tung YC, Chang FC (2006) J Appl Polym Sci 100:1146
119. Reeve MS, McCathy SP, Downey MJ, Gross RA (1994) Macromolecules 27:825
120. Kikkawa Y, Abe H, Iwata T, Doi Y (2001) Biomacromolecules 2:940
121. Eastmond GC (1999) Adv Polym Sci 149:223
122. Li S, Liu L, Garreau H, Vert M (2003) Biomacromolecules 4:372
123. Li XD, Goh SH (2002) Macromol Chem Phys 203:2334
124. Li XD, Goh SH, Zheng JW (2003) J Appl Polym Sci 87:1137
125. Li XD, Goh SH (2002) Polymer 43:6853
126. Li XD, Goh SH (2002) J Polym Sci Polym Phys Ed 40:1125
127. Li XD, Goh SH (2003) J Polym Sci Polym Phys Ed 41:789
128. Li XD, Goh SH (2001) J Appl Polym Sci 81:901
129. Li JC, Fukuoka T, He Y, Inoue Y (2005) J Appl Polym Sci 97:2439
130. Hexing B, He Y, Asakawa N, Inoue Y (2004) J Polym Sci Polym Phys Ed 42:2971
131. Zhu B, He Y, Yoshie N, Inoue Y (2004) Macromolecules 37:3257
132. Li JC, He Y, Ishida K, Inoue Y (2001) Polym J 33:773
133. Li JC, He Y, Inoue Y (2001) J Polym Sci Polym Phys Ed 39:2108
134. He Y, Asakawa N, Inoue Y (2001) Macromol Chem Phys 202:1035
135. Watanabe T, He Y, Asakawa N, Yoshie N, Inoue Y (2001) Polym Int 50:463
136. Min KE, Chiou JS, Barlow JW, Paul DR (1987) Polymer 28:172
137. Guo QP (1996) Eur Polym J 32:1409
138. Goh SH, Ni X (1999) Polymer 40:5733
139. Yau SN, Woo EM (1996) Macromol Rapid Commun 17:615
140. Woo EM, Tseng YC (2000) Macromol Chem Phys 201:1877
141. Lee SC, Woo EM (2002) J Polym Sci Polym Phys 40:747
142. Kuo SW, Chan SC, Wu HD, Chang FC (2005) Macromolecules 38:4729
143. Hong BK, Kim JK, Jo WH, Lee SC (1997) Polymer 38:4373
144. Jo WH, Kwon YK, Kwon IH (1991) Macromolecules 24:4708
145. Kuo SW, Lin CL, Chang FC (2002) Macromolecules 35:278
146. Chiu CY, Chen HW, Kuo SW, Huang CF, Chang FC (2004) Macromolecules 37:8424
147. Chiu CY, Hsu WH, Yen YJ, Kuo SW, Chang FC (2005) Macromolecules 38:6640
148. Fox TG (1956) J Appl Bull Am Phys Soc 1:123
149. Gordon M, Taylor JS (1952) J Appl Chem 2:493
150. Couchman PR (1978) Macromolecules 11:1156
151. Couchman PR, Karasz PE (1978) Macromolecules 11:117
152. Couchman PR (1982) Nature 298:729
153. Couchman PR (1982) Macromolecules 15:770
154. Kwei TK (1984) J Polym Sci Polym Lett 22:307
155. Wang J, Cheung MK, Mi Y (2001) Polymer 42:3087
156. Hsu WP (2002) J Appl Polym Sci 83:1179
157. Hsu WP, Yeh CF (1997) J Appl Polym Sci 73:431
158. Mugica A, Calahorra ME, Cortazar M (2002) Macromol Chem Phys 203:1088
159. Huang XD, Goh SH, Lee SY, Zhao ZD, Wong MW, Huan CHA (1999) Macromolecules 32:4327
160. Goh SH, Lee SY, Luo XF, Wong MW, Tan KL (2001) Macromol Chem Phys 202:31
161. Huang JY, Li XQ, Guo QP (1997) Eur Polym J 33:659
162. Kuo SW, Shih CC, Shieh JS, Chang FC (2004) Polym Int 53:218
163. Cesteros LC, Meaurio E, Katime I (1993) Macromolecules 26:2323
164. Huang MW, Kuo SW, Wu HD, Chang FC, Fang SY (2002) Polymer 43:2479
165. Zhong ZK, Guo QP (1996) Polym Int 41:315
166. Chen FL, Pearce EM, Kwei TK (1988) Polymer 29:2285
167. Lin P, Clash C, Pearce EM, Kwei TK, Aponte MA (1988) J Polym Sci Polym Phys 26:603
168. Coleman MM, Xu Y, Painter PC (1994) Macromolecules 27:127
169. Serman CJ, Painter PC, Coleman MM (1991) Polymer 32:1049
170. De Gennes PG (1979) Scaling concept in polymer physics. Cornell University Press, Ithaca
171. Kuo SW, Xu H, Huang CF, Chang FC (2002) J Polym Sci Polym Phys Ed 40:2313
172. Kuo SW, Chang FC (2003) Polymer 44:3021
173. Kuo SW, Kao HC, Chang FC (2003) Polymer 44:6873
174. Chen JK, Kuo SW, Kao HC, Chang FC (2005) Polymer 46:2354
175. Kao HC, Kuo SW, Chang FC (2003) J Polym Res 10:111
176. Yuichi K (1997) J Appl Polym Sci 63:363
177. Otsu T, Motsumoto T (1990) Polym Bull 23:43
178. Braun D, Czerwinski WK (1987) Makromol Chem 188:2389
179. Dong S, Wang Q, Wei Y, Zhang Z (1999) J Appl Polym Sci 72:1335
180. Mishra A, Sinha TMJ, Choudhary V (1998) J Appl Polym Sci 68:527
181. Schltz AR, Beach DM (1974) Macromolecules 7:902
182. Prest WM, Porter RS (1972) J Polym Sci A-2 10:1639
183. deAraujo MA, Stadler R, Cantow HJ (1988) Polymer 29:2235
184. Kuo SW, Huang CF, Tung PH, Huang WJ, Huang JM, Chang FC (2005) Polymer 46:9348
185. Huang CF, Kuo SW, Lin FJ, Chang FC (2006) Polymer 47:7060
186. Lin CL, Chen WC, Liao CS, Su YC, Huang CF, Kuo SW, Chang FC (2005) Macromolecules 38:6435
187. Kuo SW, Huang CF, Lu CH, Chang FC (2006) Macromol Chem Phys 207:2006
188. Kuo SW, Huang CF, Chang FC (2001) J Polym Sci: Polym Phys Ed 39:1348
189. Kuo SW, Lin CL, Wu HD, Chang FC (2003) J Polym Res 10:87
190. Huang CF, Kuo SW, Lin HC, Chen JK, Chen YK, Xu H, Chang FC (2004) Polymer 45:5913
191. Kuo SW, Huang WJ, Huang CF, Chan SC, Chang FC (2004) Macromolecules 37:4164

192. Li XD, Goh SH (2003) J Polym Sci Polym Phys Ed 41:789
193. Rocco AM, Fonseca CP, Loureiro FAM (2004) Solid State Ionics 166:115
194. Rocco AM, Da Fonseca CP, Pereira RP (2002) Polymer 43:3601
195. Rocco AM, Pereira RP, Felisberti MI (2001) Polymer 42:5199
196. Wu HD, Chu PP, Ma CCM, Chang FC (1999) Macromolecules 32:3097
197. Coleman MM, Yang X, Painter PC, Graf JF (1992) Macromolecules 25:4414
198. Coleman MM, Serman CJ, Bahwagar DE, Painter PC (1989) Macromolecules 22:586
199. Espi E, Alberdi M, Fernandez-Berridi MJ, Iruin JJ (1994) Polymer 35:3712
200. Serman CJ, Xu Y, Painter PC, Coleman MM (1991) Polymer 32:516
201. Espi E, Alberdi M, Iruin JJ (1993) Macromolecules 26:4586
202. Nishi T, Wang TT (1975) Macromolecules 8:909
203. Hoffman JD, Weeks JJ (1965) J Chem Phys 42:4301
204. Juana R, Cortazar M (1993) Macromolecules 26:1170
205. Painter PC, Shenoy SL, Bhagwagar DE, Fishburn J, Coleman MM (1991) Macromolecules 24:5623
206. Hoffman JD, Miller RL (1997) Polymer 38:3151
207. Flory PJ (1949) J Chem Phys 17:223
208. Talibuddin S, Wu L, Runt J, Lin JS (1996) Macromolecules 29:7527
209. Xing P, Ai X, Dong L, Feng Z (1998) Macromolecules 31:6898
210. DeJuana R, Cortazar M (1993) Macromolecules 26:1170
211. Li W, Yan R, Jing X, Jiang B (1992) J Macromol Sci, Phys B31:227
212. Hoffman JD, Weeks JJ (1962) J Res Natl Bur Stand A Phys Chem 66A:13
213. Zhong Z, Guo Q (2000) Polymer 41:1711
214. Xing P, Dong L, An Y, Feng Z, Avella M, Martuscelli E (1997) Macromolecules 30:2726
215. An Y, Dong L, Li G, Mo Z, Feng Z (2000) J Polym Sci Polym Phys Ed 38:1860
216. Kumar SK, Colby RH, Anastasiadis H, Fytas G (1996) J Chem Phys 105:3777
217. Zhang X, Takegoshi K, Hikichi K (1991) Macromolecules 24:5756
218. Li D, Brisson J (1996) Macromolecules 29:868
219. Dong J, Ozaki Y (1997) Macromolecules 30:286
220. McBrierty VJ, Douglass DC (1981) J Polym Sci Macromolecule Review 16:295
221. Demco DE, Johansson A, Tegenfeldt J (1995) J Solid State Nucl Magn Reson 4:13
222. Clauss J, Schmidt-Rohr K (1993) Acta Polymer 44:1
223. Kuo SW, Chan SC, Chang FC (2004) J Polym Sci Polym Phys Ed 42:117